Feasibility of Reconstructing Climate in Hawai'i Using Dendrochronology

A THESIS SUBMITTED TO
THE GLOBAL ENVIRONMENTAL SCIENCE
UNDERGRADUATE DIVISION IN PARTIAL FULFILLMENT
OF THE REQUIREMENTS FOR THE DEGREE OF

BACHELOR OF SCIENCE

IN

GLOBAL ENVIRONMENTAL SCIENCE

Spring 2016

By
Ryan R. Ueunten

Thesis Advisors

Rosanna A. Alegado
Axel Timmermann

We certify that we have read this thesis and that, in our opinion, it is satisfactory in scope and quality as a thesis for the degree of Bachelor of Science in Global Environmental Science.

THESIS ADVISORS

ROSANNA A. ALLEGADO
Department of OCEANOGRAPHY

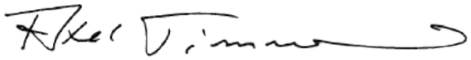

AXEL TIMMERMANN
Department of OCEANOGRAPHY

For all my friends and family that have supported me along the way. You are the inspiration for all of this.

ACKNOWLEDGEMENTS

First of all, I wish I could thank all the tremendous people who have some way supported and inspired me to get to where I am today. I know I would not have gotten this far without all of your help. With that said, I would like to acknowledge the individuals who have been there for me since the beginning. Dr. Alegado, thank you so much for your continuous guidance, sacrifice, patience, and compassion. You have done so much for me, that I couldn't possibly list everything. You have always driven me to be the best student I can be, and I truly appreciate that. Dr. Timmermann, thank you so much for taking a chance on someone like me who in the beginning, knew very little about climate or really anything. You always found the time to help me out and I am so grateful for that. I can't think of a better person to guide me on this project and it was truly an honor to work with you. Honestly, I am so lucky to have two incredible mentors and friends. Both you have taught me so many valuable things that I know I will take with me into the next journey of my life.

This project would not have been possible without the generous support from the Joint Institute for Marine Atmospheric Research (NOAA) and the Pacific Island Climate Science Center (USGS). Lastly, much thanks to Aka Beebe, Dr. Ed Cook, Dr. Niklas Schneider, Isaiah Smith and his father "Uncle" Davis Smith, Paul Chang, Aunty Davianna McGregor, Uncle Emmett Aluli, Cassius and Leihiwa Kong for assisting me at some point throughout this project. You were all an essential part of this project.

ABSTRACT

Dendrochronology, a method of analyzing annual tree ring growth to study past climates, is commonly used throughout the world (Cook & Jacoby, 1977; Gonzalez-Elizondo et al., 2005; Woodhouse et al., 2002; Li et al., 2011; Griffin et al., 2011; Worbes, 1999; Brienen & Zuidema, 2005). However, few dendrochronological studies have been conducted in Hawai‘i (Samuelson et al., 2013; Fransisco et al., 2015), where strong temperature seasonality is not prevalent. I assess the application of dendrochronology in Hawai‘i by investigating if (1) introduced conifers can produce annual tree rings and (2) if a relationship between annual tree ring growth and climate (i.e. temperature, rainfall, and cloud cover) exists. In addition, I investigate whether tree ring growth is sensitive to El Niño events. After digitally analyzing 17 tree cores collected from Hawai‘i Island, 2 out of 6 sampled trees (33%) had years of first growth match the planting years recorded in the forestry logs, thus indicating annual tree ring production. Moreover, there was an indication that two species (*Cryptomeria japonica* and *Pseudotsuga menziesii*) at two windward sites had corresponding tree ring growth. However, there were no strong and significant correlations between tree ring growth and temperature, rainfall, and cloud cover. Furthermore, tree ring growth did not respond to a combination of temperature, rainfall, and cloud cover as tested by a multiple linear regression model. Lastly, tree ring growth did not respond to strong El Niño events. Future studies should investigate the relationship between climate and tree ring growth in Hawai‘i.

TABLE OF CONTENTS

LIST OF TABLES

LIST OF FIGURES

1.0 INTRODUCTION

1.1 The Importance of Implementing Dendrochronology in Hawai‘i

As one of the most isolated places in the world, the Hawaiian Islands contain a diversity of ecosystems that are vulnerable to a changing climate (Vorsino et al., 2014; Fortini et al., 2013; Ziegler, 2002). Especially with a disproportionately large amount of native taxa in Hawai‘i federally listed as endangered or threatened (USNARA, 2014), the need to prepare for future climate changes is not only urgent but necessary. Thus, one way to prepare for future climate changes is to better our understanding of climate in Hawai‘i.

One of the most prevalent ways that climate has been recorded and analyzed in Hawai‘i is through the vast network of rain gauge stations located historically throughout the islands (Giambelluca et al., 2013, Taliaferro, 1961). Though other records such as air temperature, relative humidity, soil temperature, solar radiation, evaporation, sunshine duration, surface wind speed and direction have been collected at various sites and durations throughout the islands, the extent of available rainfall records greatly surpasses that of any other climatological records in Hawai‘i (Taliaferro, 1961).

However, relying on rain gauge stations comes with inherent shortcomings. For example, rain gauge stations require consistent maintenance, funding, and a dense spatial extent. Moreover, inconsistencies and errors in the rainfall records throughout the decades are a common issue (i.e. multiple names of the same rain gauge station, relocation of instruments, changes in instrumentation and observers) (Taliaferro, 1961; Giambelluca et al., 2013). As a result, an appreciable amount of spatiotemporal rainfall and other climatological data in Hawai‘i are sporadic and unreliable. Therefore, I emphasize that

along with instrumental data, alternative ways, such as dendrochronology, should be implemented to better characterize the climate of Hawai‘i. Other studies have utilized cores collected from inland sediments (Uchikawa et al., 2010) and coral reefs (Rooney et al., 2004) to analyze paleoclimates in Hawai‘i on a millennial timescale. In this study, I assess the applicability of analyzing tree ring growth from tree cores to study paleoclimates in Hawai‘i on a decadal timescale.

1.2 What is Dendrochronology?

The fundamental concept of dendrochronology in paleoclimate studies is quite straightforward: tree growth is directly responsive to the surrounding environmental conditions, which, in turn, are linked to local climatic influences (i.e. precipitation, temperature, photoavailability) (Cook & Jacoby, 1977; Worbes, 2002; Stahle, 1999). Therefore, the chronological growth of trees is analyzed to infer local climate variations. Specifically, dendrochronological studies infer local climate by focusing on the growth of tree rings, which are found within the wood section of tree trunks.

Certain trees, specifically conifers, are known to produce distinct tree rings annually in response to seasonality within each year of tree growth (Grissno-Mayer, 1993). There are two sections to an annual tree ring: early wood (lighter colored section) and late wood (darker colored section). Early wood forms during the fastest growing period of the year, which is typically during wet, warm months. Then, following the growth of early wood is the growth of late wood. Late wood forms as tree growth slows down, which typically occurs at the onset of cold, dry months. Eventually, tree ring growth reaches dormancy until early wood forms again when warm, wet conditions return typically during

the following year. Thus, a large annual tree ring width is possibly driven by an enhanced growing period (i.e. increased rainfall and temperature within the year), whereas a short tree ring width indicates a reduced growing period (i.e. decreased rainfall and temperature within the year). Ultimately, measuring the variations in annual tree ring widths reveals the variations in annual local climate throughout the lifespan of a tree. This means that dendrochronology can be a useful approach to reconstructing local climate, especially for times when rain gauges or weather stations were not present.

1.3 Dendrochronology in the Tropics

As more refined analytical and statistical techniques emerge, dendrochronology is becoming increasingly powerful at revealing climate variations and phenomena (Li et al., 2011). For example, dendrochronology has been implemented to analyze seasonal variations in rainfall (Worbes, 1999) and past drought events (Woodhouse et al., 2002; Cook & Jacoby., 1977). Furthermore, dendrochronology has also been used to identify the frequency of large-scale climactic phenomena such as El Niño Southern Oscillation (ENSO) events (Li et al., 2011; Worbes, 2002), Pacific Decadal Oscillation (PDO) events (Li et al., 2011), and North American monsoonal events (Griffin et al., 2011).

Despite the ubiquitous use of dendrochronology throughout the world (Cook & Jacoby, 1977; Gonzalez-Elizondo et al., 2005; Woodhouse et al., 2002; Li et al., 2011; Griffin et al., 2011; Worbes, 1999; Brienen & Zuidema, 2005) until recently, no climate related dendrochronological studies have been conducted in Hawai‘i (Samuelson et al., 2013; Francisco et al., 2015). Because annual tree ring formation is associated with distinct seasonality, Francisco et al. (2015) and Worbes (2002) have stated that majority of

dendrochronological research has been conducted in latitudes outside the tropics. However, numerous tree growth studies in tropical regions, including the studies conducted in Hawai‘i, have revealed that certain trees can produce annual tree rings. Furthermore, some studies suggest that intra-annual variations in precipitation and inundation events can drive the production of annual tree rings for certain tropical trees (Worbes, 2002; Worbes, 1999; Brienen & Zuidema, 2005). Thus, the purpose of this study is to assess if annual tree ring production is possible in Hawai‘i and also to investigate possible climate variables that can influence the production of annual tree rings.

When conducting dendrochronological studies in the tropics, Stahle (1999) suggests to select tree species that are closely related to those that are known to produce annual tree rings elsewhere. Because coniferous trees are used extensively in dendrochronological studies around the world (Worbes, 2002; Woodhouse et al., 2002; Cook et al., 1977; Li et al., 2011; Griffin et al., 2011), conifer trees naturalized in Hawai‘i were specifically selected for this study. First introduced to Hawai‘i in the late 19th Century for plantation, lumber, ranching and ornamental interests (Little Jr. & Skolmen, 1989), I investigate if conifers are useful trees for dendrochronological studies in Hawai‘i.

1.4 Case Study: Identifying El Niño in Hawai‘i Using Dendrochronology

Seasonality in Hawai‘i is commonly associated with two periods, a wet period (November through April) and a dry period (May through October) (Ziegler, 2002). Note, however, not all sites in Hawai‘i (i.e. Kona, Hawai‘i) experience this common seasonal rainfall pattern (Giambelluca et al., 2013). Nevertheless, during normal, non El Niño years, majority of annual rainfall in Hawai‘i occurs during the wet period due to enhanced trade

wind induced rainfall, the occurrence of low level convergence around the islands, and subtropical cyclonic activity (Diaz & Giambelluca, 2012; Ziegler, 2002). However, El Niño events disrupt the normal rainfall patterns in Hawai‘i resulting in reduced rainfall during the wet period. Chu (1995) outlines the mechanism behind this disruption of rainfall accordingly: As anomalously warm seawater shifts toward the central and eastern equatorial Pacific, a stronger Hadley circulation develops due to greater convection. Because Hawai‘i is geographically situated on the sinking branch of the Hadley circulation, conditions favorable for the development of precipitation are suppressed. Furthermore, during El Niño events, a stronger than average eastward extending sub-tropical jet stream occurs over Hawai‘i. Consequently, divergence occurs at the upper troposphere, resulting in less than normal precipitation (Chu, 1995).

In contrast to the wet period, a wetter than normal dry period is typically associated with El Niño in Hawai‘i (Chen, 2003). Diaz and Giambelluca (2012) state that wetter than normal dry periods in Hawai‘i tend to be associated with more localized anomalous circulation, such as near surface cyclonic activity and northward flow from the Intertropical Convergence Zone (ITCZ). Moreover, Diaz and Giambelluca (2012) observed that these wetter than normal dry periods tended to occur at the beginning or near the end of El Niño events.

Overall, El Niño manifests greater dominance during the wet period than during the dry period (Chen, 2003; Chu, 1995, Diaz and Giambelluca, 2012). In fact, Chen (2003) states that only few weather station data exhibit significant differences (80-95% confidence) in rainfall between El Niño summers and normal summers. Thus, a lower than average annual precipitation occurs during El Niño years. Because El Niño has such a

significant imprint on climate in Hawai‘i, I utilize the El Niño phenomenon as a case study to see if tree ring growth of conifers in Hawai‘i is influenced by El Niño occurrences. So, to summarize the goals of this study: (1) I assess if conifers in Hawai‘i can produce annual tree rings, then (2) I test if there is significant relationship between climate (rainfall, temperature, and cloud cover) and annual tree ring growth, and lastly (3) I examine if tree ring growth of conifers responds to El Niño events.

1.5 Hypotheses

(1) Introduced coniferous trees in Hawai‘i can produce annual tree rings because they are capable of producing annual tree rings elsewhere and also there is enough seasonality at certain places in Hawai‘i to drive annual tree ring production.

(2) In Hawai‘i, there are positive correlations between annual tree ring growth and annual rainfall and between annual tree ring growth and annual temperature because increases in both rainfall and temperature result in longer and stronger growing periods in the year.

(3) There is a negative correlation between cloud cover (measured as Total Cloud Fraction) and annual tree growth because increased cloud cover would likely hinder the photoavailability and limit tree growth.

(4) Rainfall has a relatively stronger correlation with tree ring growth than correlations between any of the other climate variables with tree ring growth. Because rainfall generally has more intra-annual variability in the tropics and has been associated with annual tree ring production in other dendrochronological studies in the tropics (Stahle, 1995; Worbes, 1999; Worbes, 2002), rainfall should have the strongest relationship with

tree ring growth in Hawai‘i.

(5) Tree ring growth is reduced during El Niño years because El Niño reduces rainfall during the wet periods in Hawai‘i. Thus, a lack of rainfall during the wet periods results in a reduced growth period for trees.

2.0 METHODS

2.1 Core Collection and Site Description

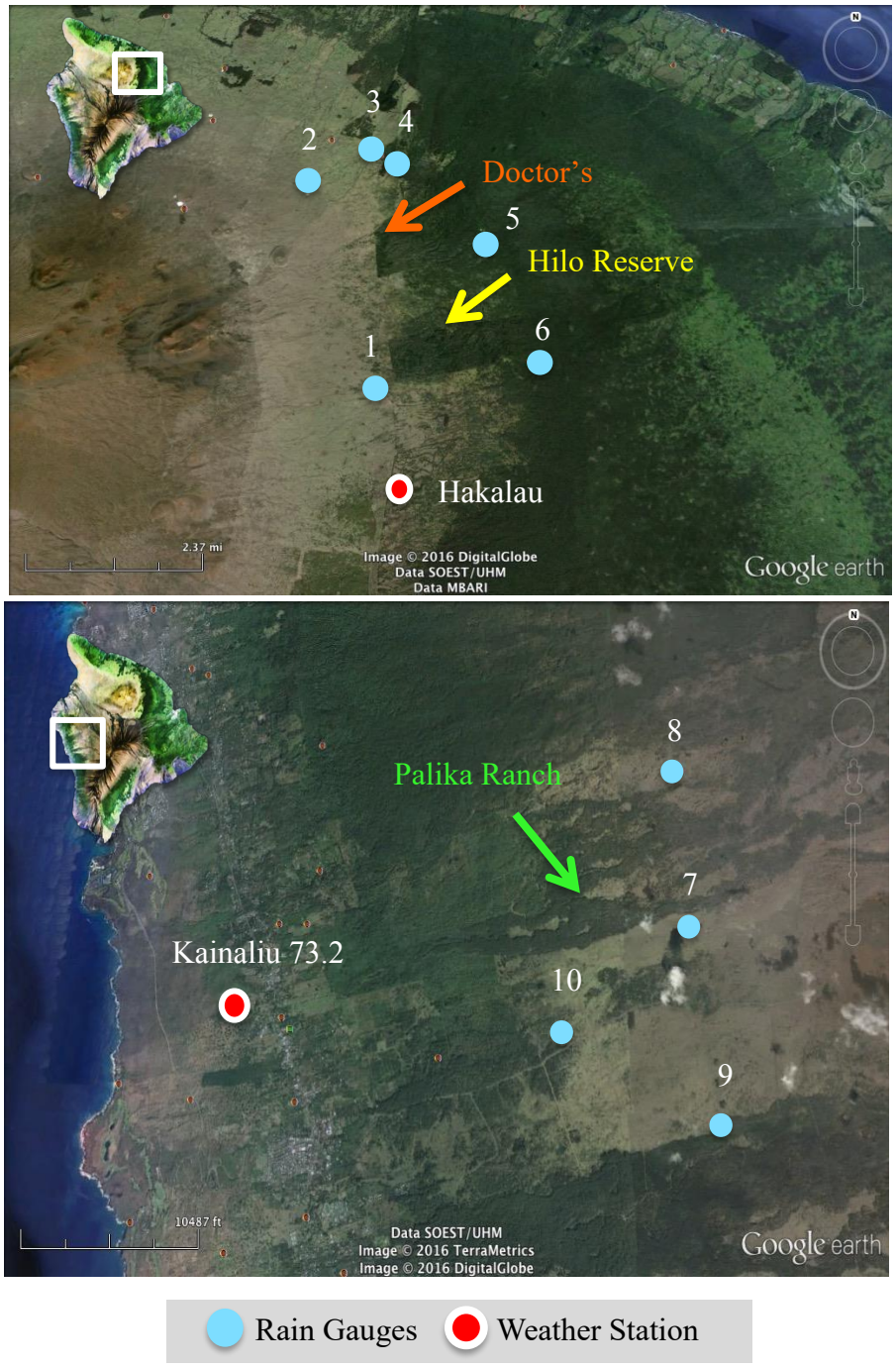

Figure 1: Locations of Sampling Sites (Top) the two windward sampling sites (Hilo Reserve and Doctor's Pit). (Bottom) the leeward sampling site (Palika Ranch). Also shown are the labeled rain gauge stations used for rainfall correlations and the weather stations used for temperature correlations.

In August 2015, 10 coniferous trees were cored at three sites on Hawai‘i Island. The three sampling sites included two windward locations (Hilo Reserve and Doctor's Pit) and one leeward location (Palika Ranch) (Figure 1 & Table 1). Specifically, 4 trees (*Cryptomeria japonica*) were cored in the western portion of the Hilo Forest Reserve, 4 trees (2 *Pseudotsuga menziesii* and 2 *Cupressussp*.) were cored at Doctor's Pit (DP), and 2 trees (*Cryptomeria japonica*) were cored at Palika Ranch.

	Hilo Reserve	Doctor's Pit	Palika Ranch
Coordinates	19.8709 N, 155.3356 W	19.8885 N, 155.3383 W	19.5531 N, 155.8734 W
Windward/Leeward	Windward	Windward	Leeward
Elevation (m)	1844	1883	1071
Species (trees sampled, number of cores)	*Cryptomeria japonica* (4 trees, 6 cores)	*Pseudotsuga menziesii* (2 trees, 4 cores) *Cupressus sp.* (2 trees, 3 cores)	*Cryptomeria japonica* (2 trees, 4 cores)
Annual Mean Rainfall Total (mm) from 1920-2007 (Giambelluca et al., 2013)	1804.9	1867.8	1179.3
Intra Annual Rainfall Range (mm) from 1920-2007 (Giambelluca et al., 2013)	69.8-230.4	77.2-234.9	66.4-130.9
Annual Mean Temperature (°C) (Zhang et al., 2016)	9.7	10.5	15.4
Intra Annual Temperature Range (°C) (Zhang et al., 2016)	9.2-10.4	10.0-11.2	14.8-16.1

Table 1: **Sampling Site Description** Three sampling sites of Hawai'i Island: Hilo Reserve, Doctor's Pit, and Palika Ranch.

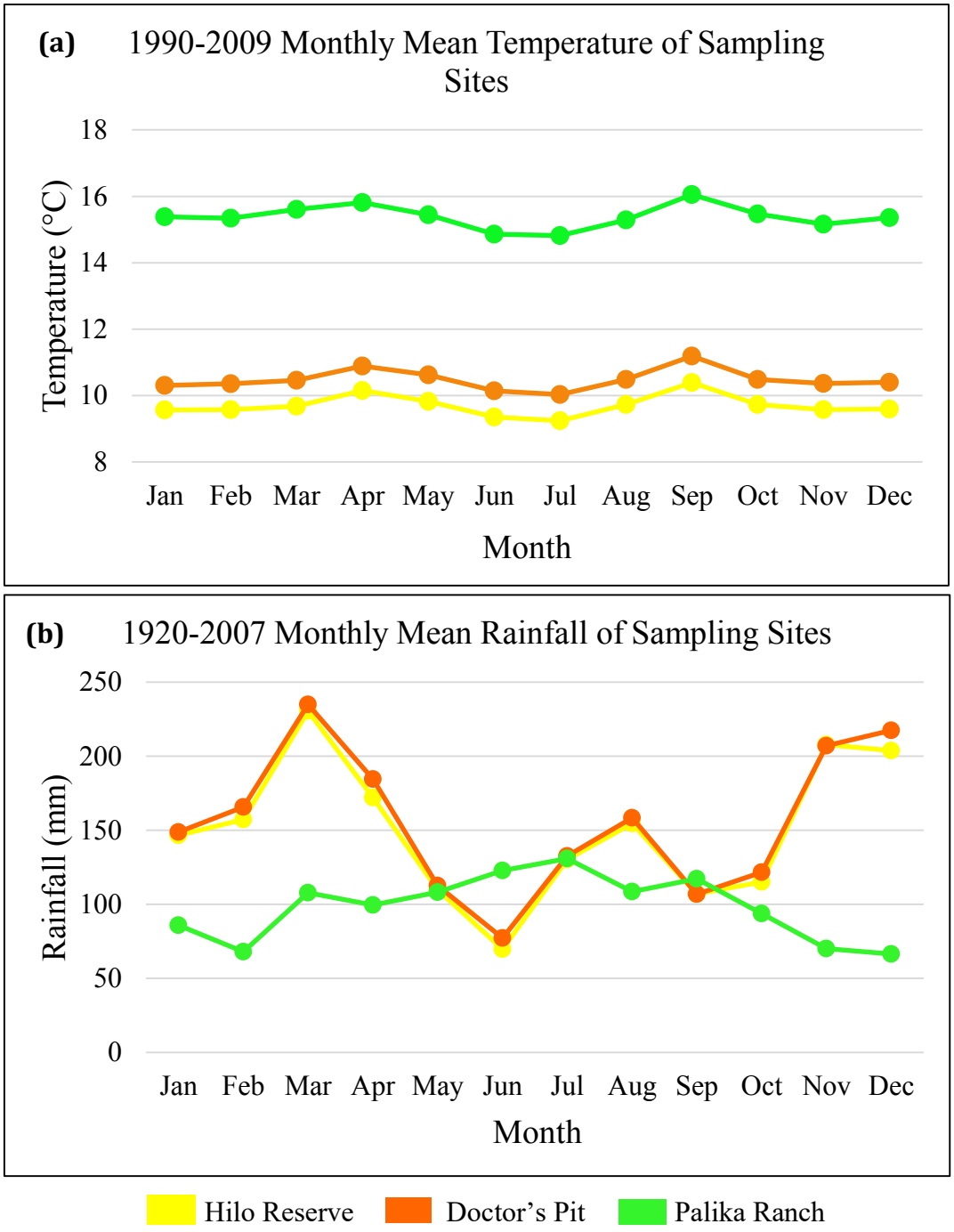

Figure 2: (a) Monthly Mean Temperature & (b) Monthly Mean Rainfall of Sampling Sites Temperature data provided by Zhang et al. (2016) and Rainfall data provided by Giambelluca et al. (2013).

Whereas these sites do not experience strong seasonality in temperature throughout the year (Figure 2a), these sampling sites were specifically targeted because they experience clear seasonality in rainfall (Figure 2b). In Figure 2b, rainfall at the two windward sites during the dry period (mean June rainfall at Hilo Reserve and Doctor's Pit

respectively: 69.8 mm and 77.2 mm) is about a factor of three less than rainfall during the wet period (mean March rainfall at Hilo Reserve and Doctor's Pit respectively: 230.4 mm and 234.9 mm). And at the leeward site, rainfall during the dry period (mean December rainfall: 66.4 mm) is about a factor of two less than rainfall during the wet period (mean July rainfall: 130.9 mm). Note that rainfall throughout the year is very similar at the two windward sites compared to rainfall at the leeward site. Also, Palika Ranch does not experience the typical seasonal rainfall pattern of wet winter months (November through April) and dry summer months (May through October). Along with seasonality, these three Hawai'i Island sites were selected for sampling because these areas were extensively planted with coniferous trees, which were recorded in the forestry logs (Skolmen, 1980). Furthermore, these sites were in close proximity to rain gauge stations as well as in descent distance to nearby weather stations.

For each sampled tree, a Haglof® Increment Borer (5.15 mm diameter, 500 mm long) was used to obtain tree cores following procedures detailed by Grissino-Mayer (2003). When possible, 2 cores per tree were obtained but due to wood rot and damage during extraction, a total of 17 tree cores were utilized for analysis. After a week of sampling, each tree core was well dried at room temperature (no remaining moisture or wet tree sap visible), mounted to prevent warping, and oriented so that ring structures were easily visible. Some cores cracked during extraction and later worsened during the drying process. To account for this, each broken piece was appropriately glued next to each other onto the mount. Once all the cores were mounted, the cores were sanded using 120, 180, and 400 grit sand paper and lightly swabbed with water to remove residue wood sandings.

2.2 Digitization of Tree Rings

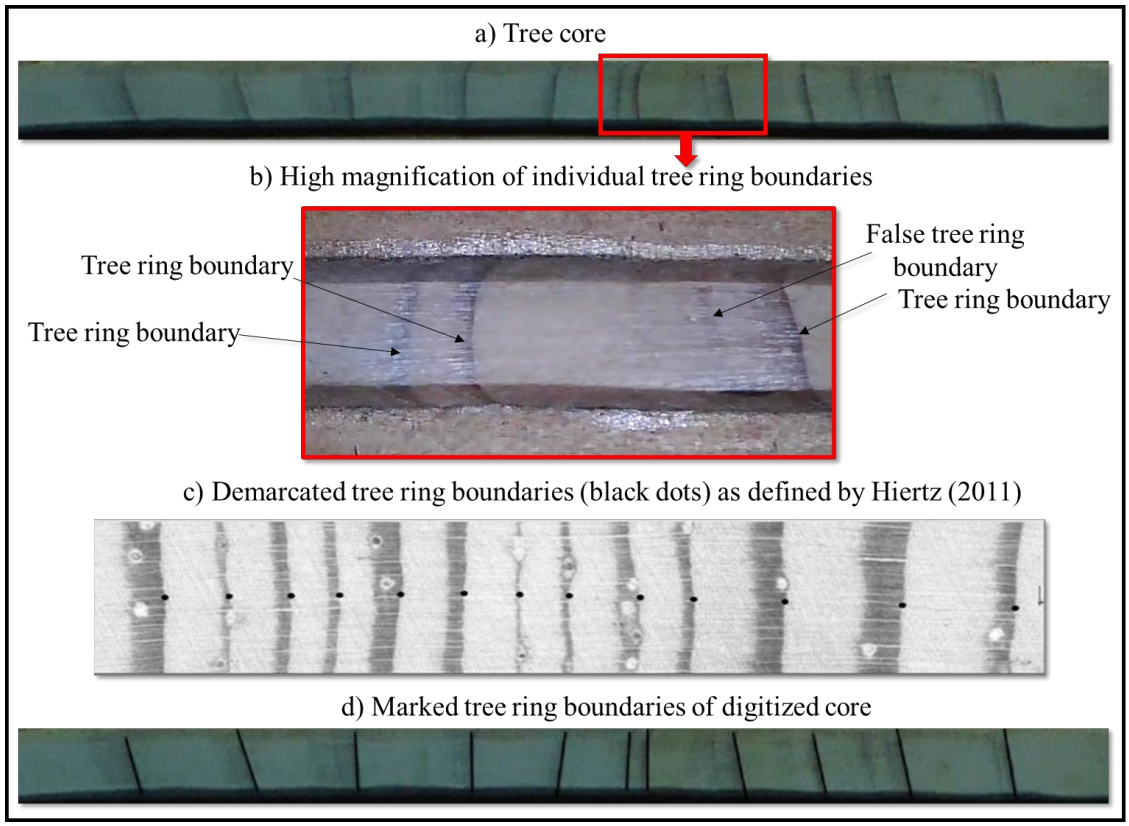

Figure 3: Tree Core Analysis Procedure and Tree Ring Boundary Identification Procedure used to identify, classify, and mark annual tree ring boundaries of tree core image.

Digitizing tree cores for dendrochronological analysis has become an emerging method of tree core analysis (Hiertz, 2011; Maxwell et al., 2011). Thus, the following is the procedure used to digitally analyze obtained tree cores. First, each core was photographed using an 18 MP Panasonic LUMIX DMC-ZS40 high-resolution camera. Then, each core image was cropped and rotated using GIMP 2.8.14 (GNU Image Manipulation Program) so that cores were horizontally straightened. To distinguish tree rings in each core image, all tree ring boundaries in each core image were marked using a 1.00 thickness black line in GIMP 2.8.14. I defined a tree ring boundary as the clear division between the end of the late wood growth and the beginning of the early wood growth (Hiertz, 2011; Maxwell et al., 2011) (Figure 3). Tree ring boundaries in each core

image were visually cross-referenced against the corresponding mounted tree core using a Celestron MicroFi Handheld Microscope. Next, all core images with marked tree ring boundaries were converted from RGB scale values into 8-bit grayscale values (0 = Black and 255 = White) using the desaturation operation in GIMP 2.8.14 and adjusted to a brightness setting of 254 units. Tree ring boundaries were re-traced as necessary.

Next, each core image was uploaded onto a MatLab script designed specifically to detect distinct differences in pixel values (i.e. where pixel grayscale values suddenly decrease below a value of 3). Because tree ring boundaries were traced in black (resulting in low grayscale values) and the brightness of the rest of the core images was increased (resulting in high grayscale values), tree ring boundaries were detected in each core image (Figure 4). Moreover, tree ring widths were measured (in pixels) and assigned calendar years. Thus, the outermost ring was assigned the year 2015, second outermost ring was assigned the year 2014, until eventually the innermost ring was the year of observed first growth.

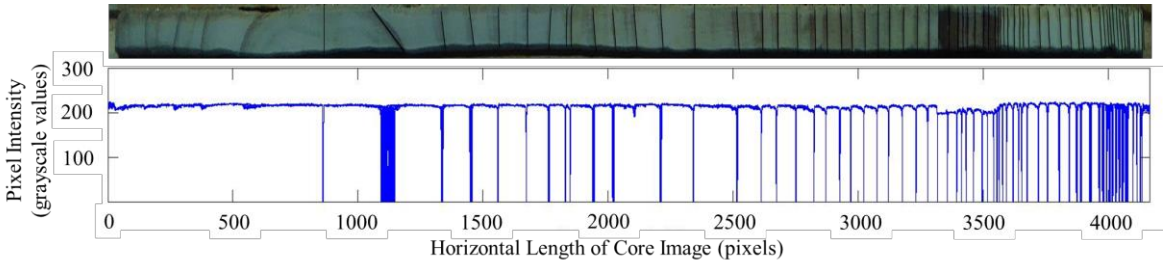

Figure 4: Detection of Tree Ring Boundaries (Below) distinct differences in pixel grayscale values (y axis) were detected along the horizontal length (x axis) of a marked core image (above).

Due to human error, most tree cores were not bored directly toward the center of the tree, resulting in distorted tree ring boundaries and tree ring width measurements. The various angles of many of the tree ring boundaries (i.e. < 90° or > 90° from the horizontal length of the core) are visual indications of distortions in the tree ring widths. Assuming each sampled tree grew cylindrically, an additional Matlab script was created to correct

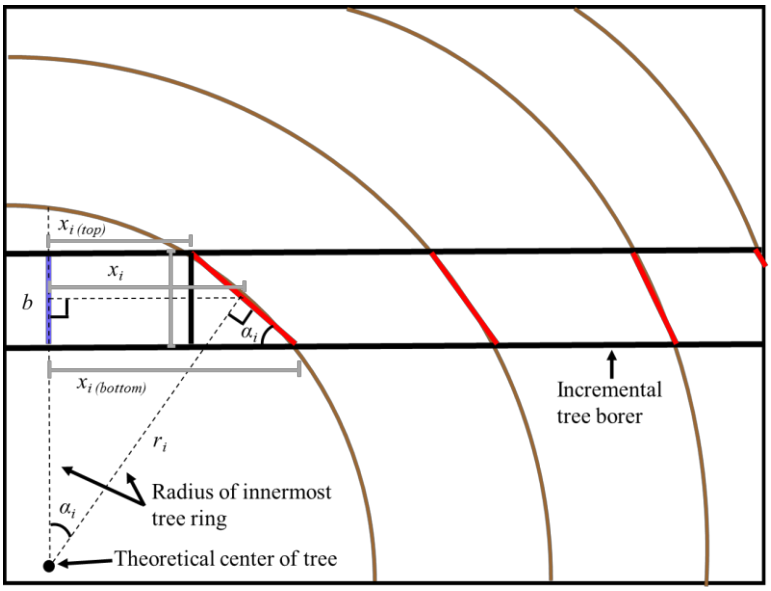

Figure 5: Core Correction Procedure A typical scenario of an incremental tree borer coring into a tree that is not oriented toward the center of the tree. The red lines represent the tree ring boundaries that are found on the core; blue line (*b*), represents the orthogonal intersection of the tree core with the radius of the innermost tree ring. Line *b* was approximately identified using the handheld microscope and determined to be the halfway point in the tree core where the late woods of consecutive tree rings grew in opposite directions.

Variables: i = the number representing a tree ring boundary in the core (i.e. $ring_1$, $ring_2$,… , $ring_i$, $ring_{i+1}$, $ring_{i+2}$,...) ; r_i = theoretical radius of a tree ring; b = line marking the orthogonal intersection between the radius of the innermost tree ring and the tree core; d = the vertical length of the tree core;α_i = angle between a tree ring boundary and the horizontal length of the core; x_i = distance from line b to the middle of a tree ring boundary; $x_{i\,(top)}$ = distance from line b to the top of a tree ring boundary (red line); $x_{i\,(bottom)}$ = distance from line b to the bottom of a tree ring boundary (red line)

distortions in each tree core image. Figure 5 shows a typical scenario of a core being extracted from a tree with the tree borer not oriented toward the center of the tree. Figure 5 additionally shows the specific lengths identified for this core correction process (x_i, $x_{i(top)}$, $x_{i(bottom)}$, and d).

Before core corrections were made, the determination of where in each core a tree started growing in opposite directions (line *b*) was required. Specifically, line *b* indicates where consecutive late woods grew in opposite directions (Figure 6). Line *b* is also defined as the orthogonal intersection between the tree core and the radius of the innermost tree ring. Thus, during the identification and marking of tree ring boundaries, line *b* was identified and marked as well (1.00 thickness black line in GIMP 2.8.14). If the location

where consecutive late woods grew in opposite directions was not determinable, line *b* was marked at the end of the core, on the side closest to the center of the tree.

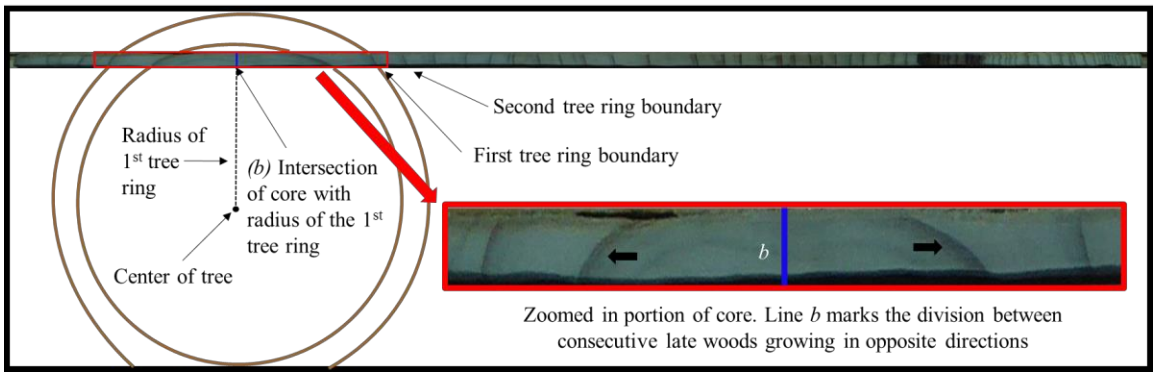

Figure 6: **Identifying Line *b*** Blue line represents line *b*. The determination of line *b* is the halfway mark of consecutive late wood growths oriented in opposite directions in the core.

This additional Matlab script obtained the lengths of x_i, $x_{i(top)}$, and $x_{i(bottom)}$ by measuring the distances of detected tree ring boundaries from line *b*. Also, the vertical length of a tree core, *d,* was obtained by measuring the distance (in pixels) from the bottom of the core image to the top of the core image. Ultimately, the values of x_i, $x_{i(top)}$, $x_{i(bottom)}$, and *d* of each core image were applied in the following algorithm:

$$If\ x_{i\,(bottom)} = x_{i\,(top)},\ then:\ r_i = x_i$$

$$If\ x_{i\,(bottom)} \neq x_{i\,(top)},\ then:\ \alpha_i = \tan^{-1}\left(\frac{d}{x_{i\,(bottom)} - x_{i\,(top)}}\right)$$

$$r_i = \frac{x_i}{\sin(\alpha_i)}$$

The outcome of this core correction process determined the radius of every tree ring of every core (r_i). Ideally, obtaining the radius of every tree ring for each tree core is essential because digitally correcting each core means that x_i will equal r_i. Thus, the corrected width values of each core were the differences between consecutive r_i values.

Figure 7 shows an example of a corrected tree core and the corresponding growth plot of the sampled tree. In each corrected core, there is a decreasing trend in tree ring

growth as the trees ages (shown in the growth plot of Figure 7). This age effect needed to be removed in order to best display tree ring growth as a response to variations in climate. Therefore, every tree ring width value was first divided by the sum of all tree ring width values in its respective core so that relative tree ring width values were produced. Then, each relative tree ring width value was subtracted and divided by the running mean

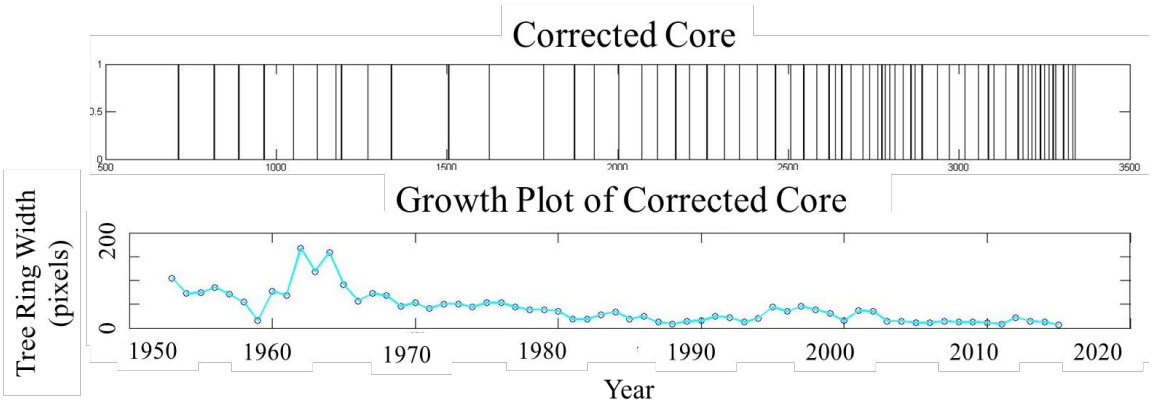

Figure 7: Corrected Tree Core Example of a corrected tree core (above) and the corresponding growth plot (below). The x axis marks the years of tree growth and the y axis indicates corrected tree ring width values of each corresponding year.

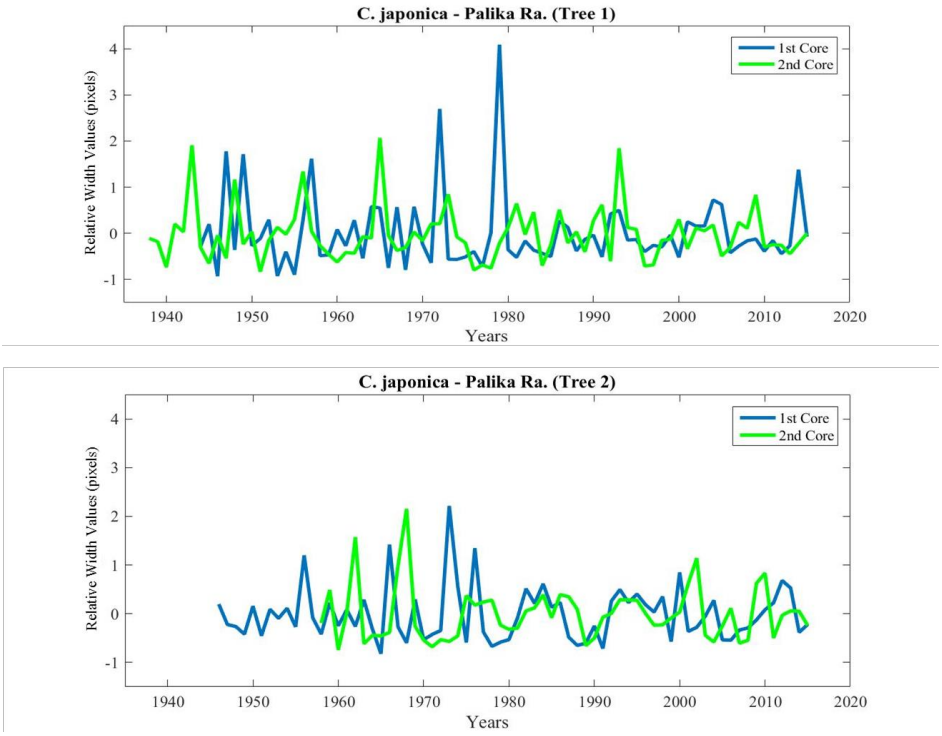

Figure 8a: Tree Growth Signals of Corrected Cores (*C. japonica* Palika Ranch) Tree ring growth of two *C. japonica* trees from Palika Ranch (4 cores). The different colors in each plot indicate different cores taken from the same tree. Anomalous, high pass tree ring width values relative to length of its core are shown (y axis) for each corresponding year of growth (x axis).

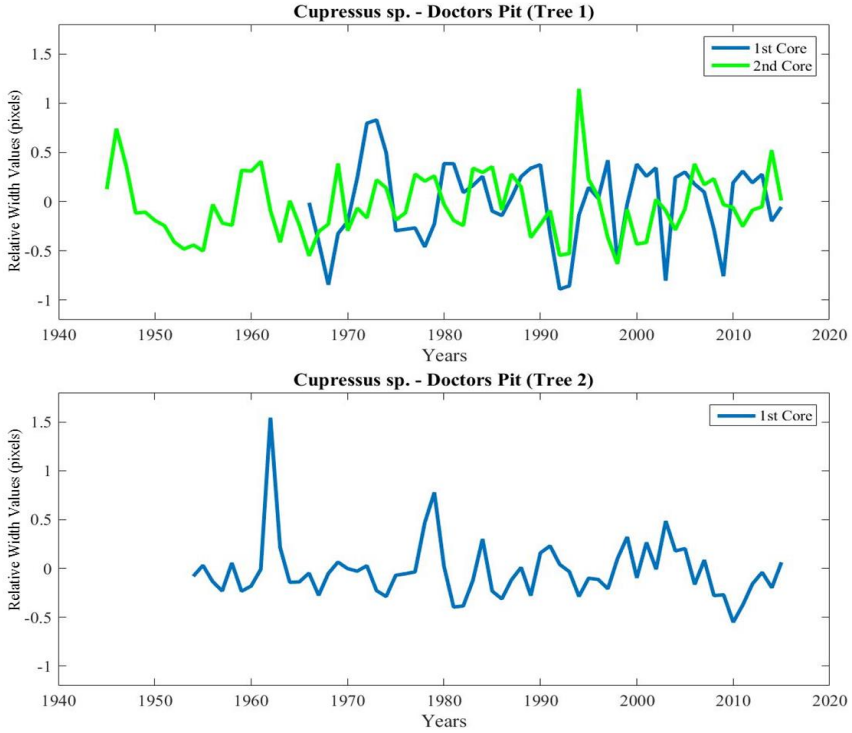

Figure 8b: Tree Growth Signals of Corrected Cores (*Cupressus sp.* Doctor's Pit) Tree ring growth of two *Cupressus sp.* trees from Doctor's Pit (4 cores). The different colors in each plot indicate different cores taken from the same tree. Anomalous, high pass tree ring width values relative to length of its core are shown (y axis) for each corresponding year of growth (x axis).

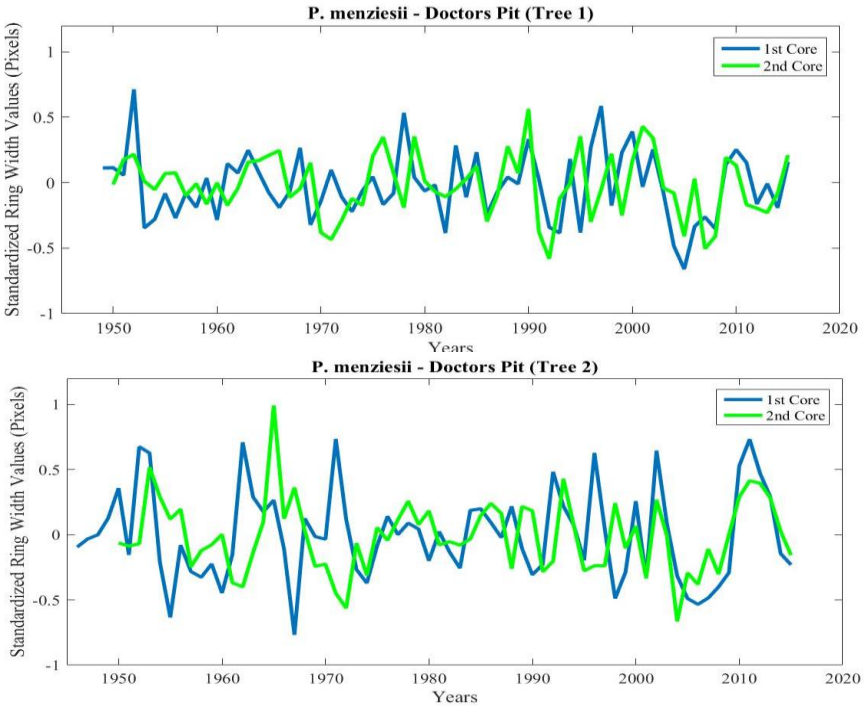

Figure 8c: Tree Growth Signals of Corrected Cores (*P. menziesii.* Doctor's Pit) Tree ring growth of two *P. menziesii.* trees from Doctor's Pit (4 cores). The different colors in each plot indicate different cores taken from the same tree. Anomalous, high pass tree ring width values relative to length of its core are shown (y axis) for each corresponding year of growth (x axis).

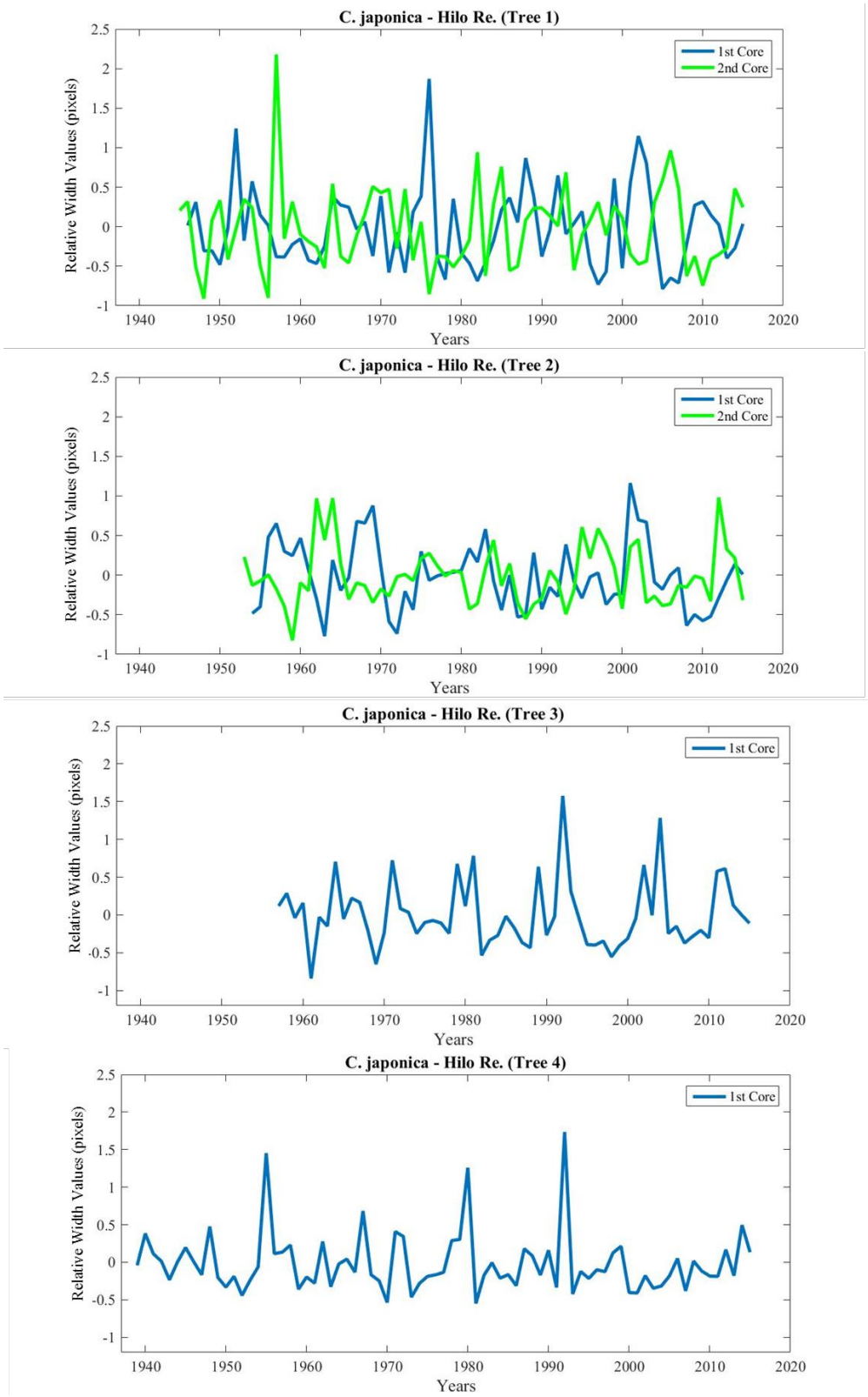

Figure 8d: Tree Growth Signals of Corrected Cores (*C. japonica* Hilo Reserve) Tree ring growth of four *C. japonica* trees from Hilo Reserve (6 cores). The different colors in each plot indicate different cores taken from the same tree. Anomalous, high pass tree ring width values relative to length of its core are shown (y axis) for each corresponding year of growth (x axis).

(window of 6) so that anomalous high pass tree width signals were produced for each tree core (Figure 8a,b,c,d). Ultimately, this procedure to digitally analyze tree ring growth (Figure 9) produced anomalous high pass tree ring width signals that best reveal fluctuations in tree ring growth with minimal influence of non-climatic trends.

Digital Tree Ring Analysis Procedure

1. Photograph each tree core
2. Crop to horizontally align tree core images
3. Identify and mark all tree ring boundaries and line *b* on each tree core image
4. Upload marked images into Matlab to measure and count tree ring widths
5. Correct each tree core to eliminate width distortions
6. Divide width values by the sum of widths in its core
7. Subtract and divide each relative width value by the running mean (window of 6)

Figure 9: Digital Tree Ring Analysis steps used to digitally analyze each tree core

2.3 Verification of Annual Tree Ring Growth

In other dendrochronological studies, all three tree species selected in our research were found to produce annual tree rings or related to species (within the same genera) that were found to produce annual tree rings (*Pseudotsuga menziesii*: Gonzalez-Elizondo, 2005; Griffin et al., 2011; *Cupressus sp.*: David et al., 2014; Yang et al., 2010; *Cryptomeria japonica*: Luong et al., 2013). After obtaining the years of observed first growth for each tree core, a range of planting years of each sampled tree was found in old forestry logs (Skolmen, 1980). This range of years was the expected years of first growth for each sampled trees. Thus, for each sampled tree, the year of observed first growth was compared with the expected range of years of first growth to determine if the sampled tree produced annual tree rings. Note, tree cores were only used if the center portion of the tree was

identified. In a tree core, the center portion of the tree was identified where consecutive late woods grew in opposite directions (same procedure as identifying line *b*).

2.4 Construction of Composite Cores

Each of the 17 tree cores were placed into one of four groups. Groups were based on tree species and site location. The first group consisted of 6 *Cryptomeria japonica* cores collected at the Hilo Reserve; the second group consisted of 4 *Pseudotsuga menziesii* cores collected at the Doctor's Pit site; the third group consisted of 3 *Cupressus sp.* cores collected at the Doctor's Pit site; and the fourth group consisted of 4 *Cryptomeria japonica* cores collected at Palika Ranch. Then, composite cores were constructed for each group to represent overall tree growth of the sampling sites based on species. A composite core was created by averaging all ring width values of tree cores in a group, starting with the first year of common growth. For example, if all the cores in a group had a width value corresponding to the year 1958, then the average of all those width values constituted the width value of the composite core corresponding to the year 1958. Ultimately, tree ring width series of four composite cores were constructed based on tree species and location: (1) *Cryptomeria japonica* - Hilo Reserve; (2) *Pseudotsuga menziesii* - Doctor's Pit (DP); (3) *Cupressus sp.*- Doctor's Pit; (4) *Cryptomeria japonica* - Palika Ranch.

2.5 Correlation of Tree Ring Growth and Rainfall

In order to test for correlation between tree ring growth and rainfall, monthly rainfall data (mm) was selected from 4 rain gauge stations located near the Palika Ranch site and from 6 rain gauge stations located near both the Hilo Reserve and Doctor's Pit sites. Spanning from 1920-2007, all rainfall data was provided by the Rainfall Atlas of

Hawai‘i (Giambelluca et al., 2013; Frazier et al., 2016). Descriptions of each selected rain gauge station are found in Table 2 and time series of rainfall recorded by selected rain gauge stations are found in Appendix 1.

First, monthly rainfall data was converted into annual rainfall data by repeatedly summing 12 consecutive monthly rainfall values together. Since the annual period that tree ring growth corresponds to was not known for each sampled tree (i.e. January – December, February – January, March – February, and so on), 12 different versions of annual rainfall were arranged. Thus, each version of annual rainfall was created by repeatedly summing January to December rainfall values, February to January rainfall values, March to February rainfall values, and so on. Next, annual anomalous rainfall values were produced by subtracting each annual rainfall value with the mean annual rainfall value. In order to

Tree Coring Site	Rain Gauge Name	Rain Gauge Number	State Key Number	Elevation (ft)	Latitude (N)	Longitude (E)
Hilo Reserve/The Doctor's Pit	HOPUWAI	1	125	6425	19.84695	-155.337
Hilo Reserve/The Doctor's Pit	IOLEHAEHAE TANKS	2	121	6300	19.90695	-155.361
Hilo Reserve/The Doctor's Pit	KEANAKOLU 1	3	124	5280	19.91695	-155.339
Hilo Reserve/The Doctor's Pit	KEANAKOLU 2	4	124.1	5280	19.91528	-155.336
Hilo Reserve/The Doctor's Pit	MAULUA/KAULUA	5	126	5140	19.88862	-155.307
Hilo Reserve/The Doctor's Pit	NAUHI GULCH	6	128	5160	19.85529	-155.297
Palika Ranch	MOMOHAA (3875)	7	74.7	3875	19.5492	-155.858
Palika Ranch	KAUKAHOKU	8	74.1	4030	19.57197	-155.859
Palika Ranch	ORCHARD	9	77.9	3750	19.52198	-155.855
Palika Ranch	KANAKAMELAI	10	29.5	3120	19.53364	-155.881

Table 2: Rain Gauges List of rain gauges used in the correlation between rainfall and tree ring growth. Rain gauge numbers correspond to Figure 1 (Giambelluca et al., 2013; Frazier et al., 2016)

represent overall annual anomalous rainfall at each sampling site, the 4 annual anomalous rainfall data recorded by rain gauge stations near Palika Ranch were averaged together and similarly, the 6 annual anomalous rainfall data recorded by rain gauge stations near both the Hilo Reserve and Doctor's Pit sites were also averaged together. Altogether, two mean annual anomalous rainfall datasets, each comprising of 12 different versions of annual rainfall, were produced. This filtering process of rainfall values implicitly matched the same process used to produce tree width values of each composite core.

Linear correlations were performed for each series of tree ring growth and a rainfall dataset of its respective sampling site. Before any correlations were made, all tree ring growth series and all annual anomalous rainfall datasets were detrended. Also, lag values ranging between -10 and 10 were implemented in each correlation in order to account for errors that might have occurred during the classification and counting process of the tree ring widths.

2.6 Correlation of Tree Ring Growth and Temperature

Monthly mean surface temperature data was obtained from two sources, the Hawaiian Regional Climate Model (Zhang et al., 2016) and from two weather stations from the Global Historical Climatology Network version 3 (GHCNv3) (Lawrimore et al., 2011) of NOAA's Climactic Data Center. The Hawaiian Regional Climate Model is a downscaled version of a larger climate forecasting model (Weather Research and Forecasting Model) and has been modified to account for specific physical characteristics of Hawai‘i (Zhang et al., 2016). Surface temperature data obtained from this model is referred to as 'model temperature data'. The surface temperature data from the two weather stations (referred to

as ‘station temperature data’) was selected based on their close proximity to the tree sampling sites. The Hakalau Station is the nearest weather station to both the Doctor’s Pit and Hilo Reserve sites and the Kainaliu 73.2 Station is the nearest weather station to the Palika Ranch site (Figure 5). Because the model temperature data spans only from 1990-2009, we utilized the station temperature data to fill in the years of 2010-2015. Adjustments (2°C corrections) were appropriately made to the station temperature data in order to account for elevational differences between the two sources of temperature data. Thus, specifying on the location of the sampling sites, two datasets of monthly surface temperature, both spanning 26 years (1990-2015), were produced.

Similar to the rainfall datasets, monthly surface temperature datasets were converted into annual surface temperature datasets. Again, 12 different versions of annual temperature data were produced in each dataset (i.e. years classified as January-December, February-January, and so on). Also, in both datasets, annual temperature values were subtracted by the mean annual temperature value to produce annual anomalous temperature datasets. Thus, one dataset represented annual anomalous temperature at the Palika Ranch site and the other dataset represented annual anomalous temperature data at the Hilo Reserve and Doctor’s Pit sites. This filtering process of temperature values implicitly matched the same process used to produce tree width values of each composite core.

Tree ring width series of each composite core were linearly correlated with annual anomalous temperature of its respective site. All tree ring width series and anomalous temperature datasets were detrended before correlations were performed. Also, lag values ranging between -10 and 10 were implemented in each cross correlation in order to account

for errors that might have occurred during the identification and counting process of the tree ring widths.

2.7 Correlation of Tree Ring Growth and Cloud Cover

Three monthly total cloud fraction datasets for the three sampling sites were obtained from the Hawaiian Regional Climate Model (Zhang et al., 2016). The three monthly total cloud fraction datasets span from the years 1990-2009 and were converted into annual total cloud fraction datasets similarly to the annual rainfall and temperature datasets. In each total cloud fraction dataset, 12 different versions of annual total cloud fraction data were produced to account for the 12 possible periods of annual tree ring growth. Furthermore, in each total cloud fraction dataset, each value was subtracted by the mean annual total cloud fraction value. This filtering process of total cloud fraction values implicitly matched the same process used to produce tree width values of each composite core. Each tree ring width series of each composite core and annual anomalous total cloud fraction datasets was detrended and cross correlated based on the same location. Lag values ranging between -10 and 10 were implemented in each cross correlation in order to account for errors that might have occurred during the classification and counting process of the tree ring widths.

2.8 Multiple Linear Regression of Tree Ring Growth

In addition to linear correlations, a multiple linear regression approach was used to test if there is relationship between annual tree ring growth and climate. Specifically, this

approach determined if annual tree ring growth of each composite cores was responsive to a combination of the three climate variables (temperature, rainfall, and cloud cover). Multiple linear regression models for each composite core were constructed (in Excel using the regression function in Data Analysis Package) to produce best fit values of annual tree ring widths (response variable: y) from corresponding yearly values of surface temperature, rainfall, and total cloud fraction (independent variables: x_1, x_2, *and* x_3). The years of 1990-2007 spanned the time frame of each model because values from all three independent variables and the response variables shared this common period.

2.9 Characterization of El Niño Events in Hawai‘i

Years of Strongest El Niño Events
1877
1878
1888
1889
1902
1941
1972
1973
1982
1983
1987
1992
1997
1998

Table 3: **Years of Strongest El Niño Events** Based on five consecutive periods in which the three-month running mean of sea surface temperature (SST) in the Niño 3.4 Region is ≥ 1.5 °C from the 1971-2000 baseline SST (NOAA, 2015). SST from ERSSTv4 (Huang et al., 2014; Liu et al., 2014; Huang et al., 2015)

Lastly, annual tree ring growth was analyzed specifically during El Niño events. The definition of an El Niño event is five consecutive periods in which the three-month running mean of sea surface temperature (SST) in the Niño 3.4 Region is ≥ 0.5 °C from the 1971-2000 baseline SST (NOAA, 2015). To find years of El Niño events, sea surface

temperature data was provided by the Extend Reconstructed Sea Surface Temperature dataset (ERSSTv4,https://www.ncdc.noaa.gov/data-access/marineocean-data/extended-reconstructed-sea-surface-temperature-ersst-v4) in the Niño 3.4 Region (5°N-5°S, 120°W-170°W) (Huang et al., 2014; Liu et al., 2014; Huang et al., 2015). Spanning from 1854-

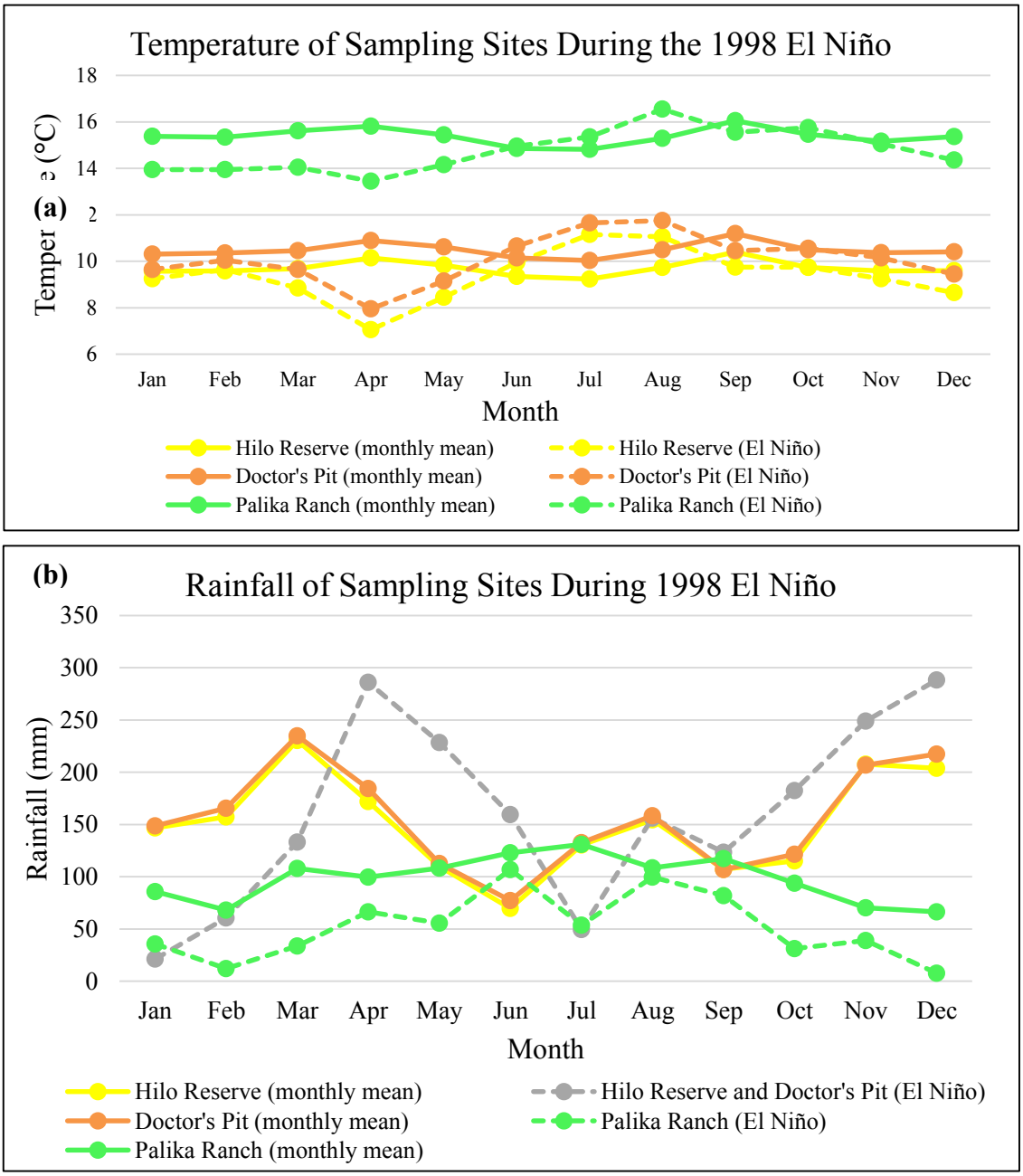

Figure 10: (a) Temperature and (b) Rainfall of Sampling Sites During 1998 El Niño Monthly mean and 1998 El Niño temperature values provided by Zhang et al., (2016). Monthly mean rainfall values provided by Giambelluca et al. (2013) and 1998 El Niño rainfall values were recorded by rain gauge stations listed in Table 2 (Giambelluca et al., 2013, Frazier et al., 2016).

Present, years of strongest El Niño events were found when by selecting a ≥ 1.5 °C departure from the baseline SST. A list of strongest El Niño years is found in Table 3.

As shown in Figure 10a and 10b, El Niño can impact the seasonal variation of temperature and rainfall at the three sampling sites. Specifically, during the 1998 El Niño event, the wet period at the two windward sites shifted by a month, and rainfall at Palika Ranch decreased overall. Moreover, seasonality in temperature at the three sampling sites during the 1998 El Niño event inversely shifted throughout the year. Lastly, intra-annual variations in rainfall and temperature at the three sampling sites increased from the mean intra-annual variation during the 1998 El Niño event. Ultimately, there is a good indication that the three sampling sites experience distinct changes in temperature and rainfall during El Niño events.

3.0 RESULTS

3.1 Annularity of Introduced Conifer Tree Ring Structures

I first hypothesized that conifers in Hawai‘i can produce annual tree rings. This was tested by comparing the years of observed first growth of collected cores (determined during the digital tree ring analysis) with the expected planting years of the sampled trees. Also, only cores with identifiable center portions of the tree were tested. For each tested core, if a year of observed first growth was within the range of expected years of first growth, then there was an indication that the sampled tree in which the core was taken from produced annual tree rings. Out of the 10 tree cores used in this analysis (representing 6 sampled trees), 2 tree cores had years of observed first growth match expected years of first growth. Furthermore, these 2 tree cores (blue and purple points in Figure 11) were from two *C. japonica* trees taken at the Hilo Reserve. Notice, however, that another core (purple point) taken from the one of these identified *C. japonica* tree did not have matching

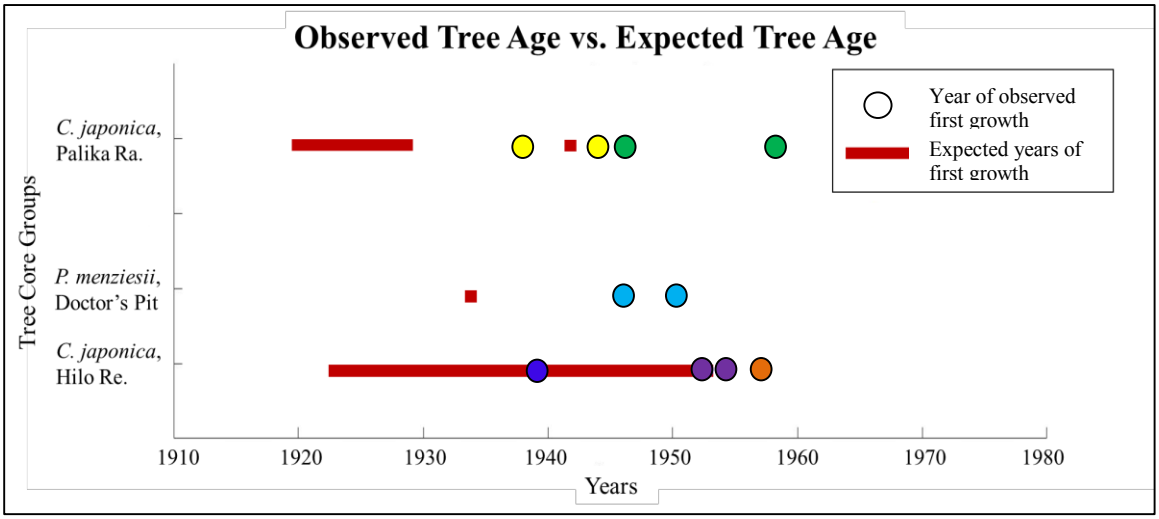

Figure 11: Observed Age vs. Expected Age of Sampled Trees Colored dots represent the years of observed first growth of cores where the center portion of the tree was identified. Dots with the same color represent cores taken from the same tree. Tree cores are grouped by tree species and sampling location (y axis). The red bars signify the expected years of first growth of our sampled trees determined by the forestry logs. Only 2 of the 10 tree cores (taken from two *C. japonica* trees from the Hilo Reserve) had matching years of observed and expected first growth. Thus, 33% of sampled tree indicated annual tree ring growth.

years of observed and expected first growth. The years of observed first growth of these two mismatching *C. japonica* cores differed by only one year (1953 and 1954). Lastly, only one year was recorded in the forestry logs as the planting date for *P. menziesii* trees at the Doctor's Pit site. This clearly limited the range of expected years of first growth for *P. menziesii* trees at the Doctor's Pit site. In the end, there was good evidence that 2 sampled trees (33%) produced annual tree rings. As for the rest of the sampled trees, the determination of annual tree ring production was inconclusive.

3.2 Tree Ring Growth of Composite Cores

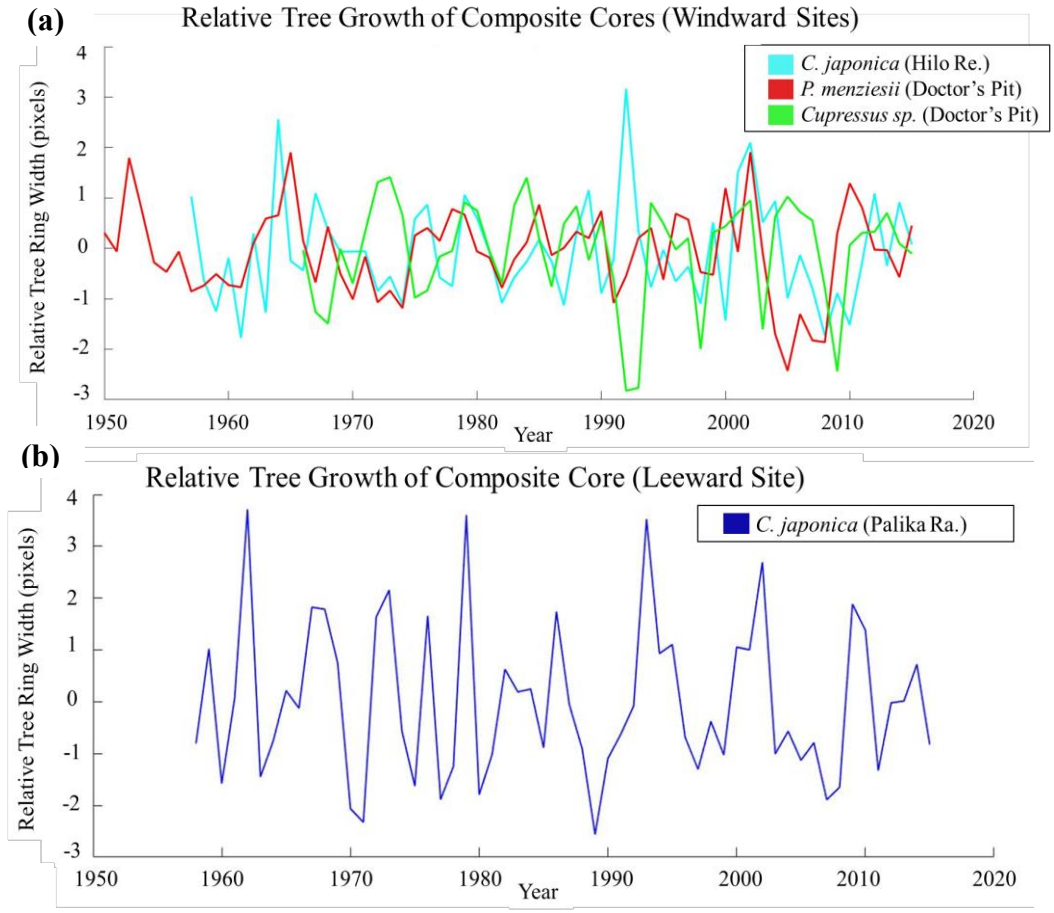

Figure 12: Relative Tree Ring Growth of 4 Composite Cores (a) The tree ring growth of 3 composite cores representing the windward sampling sites of Hawai'i Island. **(b)** The tree ring growth of one composite core representing the leeward sampling site of Hawai'i Island.

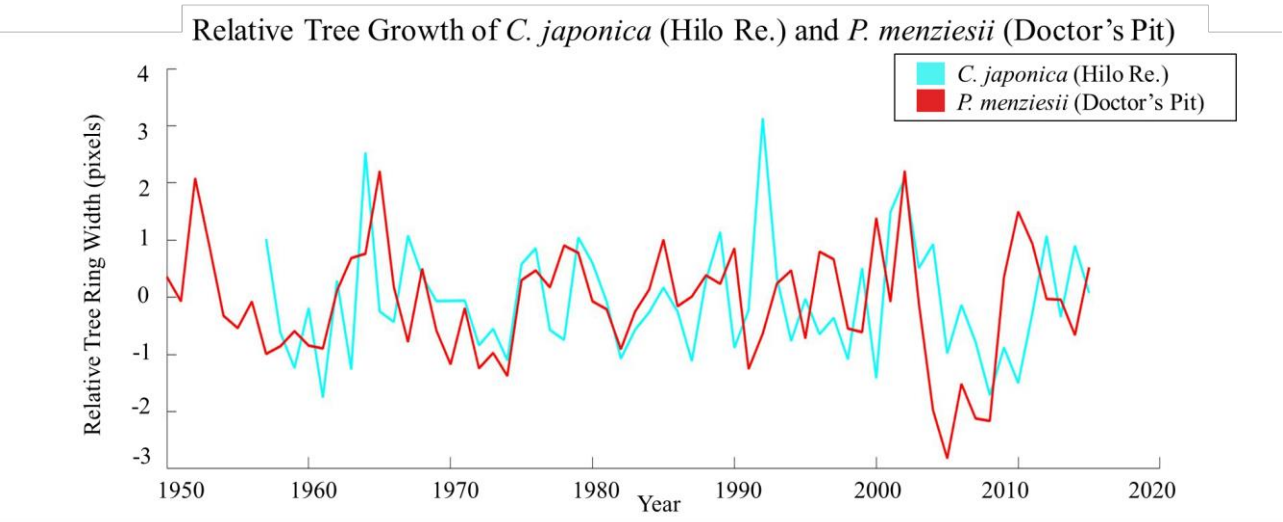

Figure 13: Relative Tree Ring Growth of *C. japonica* (Hilo Reserve) and *P. menziesii* (Doctor's Pit) Composite Cores (a) Relative tree ring widths (y axis) of two composite cores from two windward sites of Hawai'i Island. Note, there is some correspondence in tree growth of these composite cores.

Four composite cores were constructed in order to represent the best overall tree growth of each sampling site based on species. Composite cores were constructed by averaging width values of tree cores taken from the same species and sampling location. Tree ring growth of the leeward composite core (*C. japonica* - Palika Ranch) did not match well with tree ring growths of windward composite cores (*C. japonica* – Hilo Reserve, *P. menziesii* – Doctor's Pit, and *Cupressus sp.* – Doctor's Pit) (Figure 12). Although the same tree species (*C. japonica*) was sampled in both the leeward and windward sites, tree ring growth did not correspond well. Moreover, tree ring growth of *Cupressus sp.* and *P. menziesii* at the same location (Doctor's Pit) did not have corresponding tree ring growth.

However, there is some indication that tree ring growth of the *C. japonica* (Hilo Reserve) composite core corresponded with tree ring growth of the *P. menziesii* (Doctor's Pit) composite core (Figure 13). In particular, during the period of 2003-2010, tree ring growth of these two composite cores were significantly reduced. Ultimately, this suggests that a common environmental factor is influencing tree growth at these two windward sites.

3.3 Correlation Between the Climate Variables and Tree Ring Growth

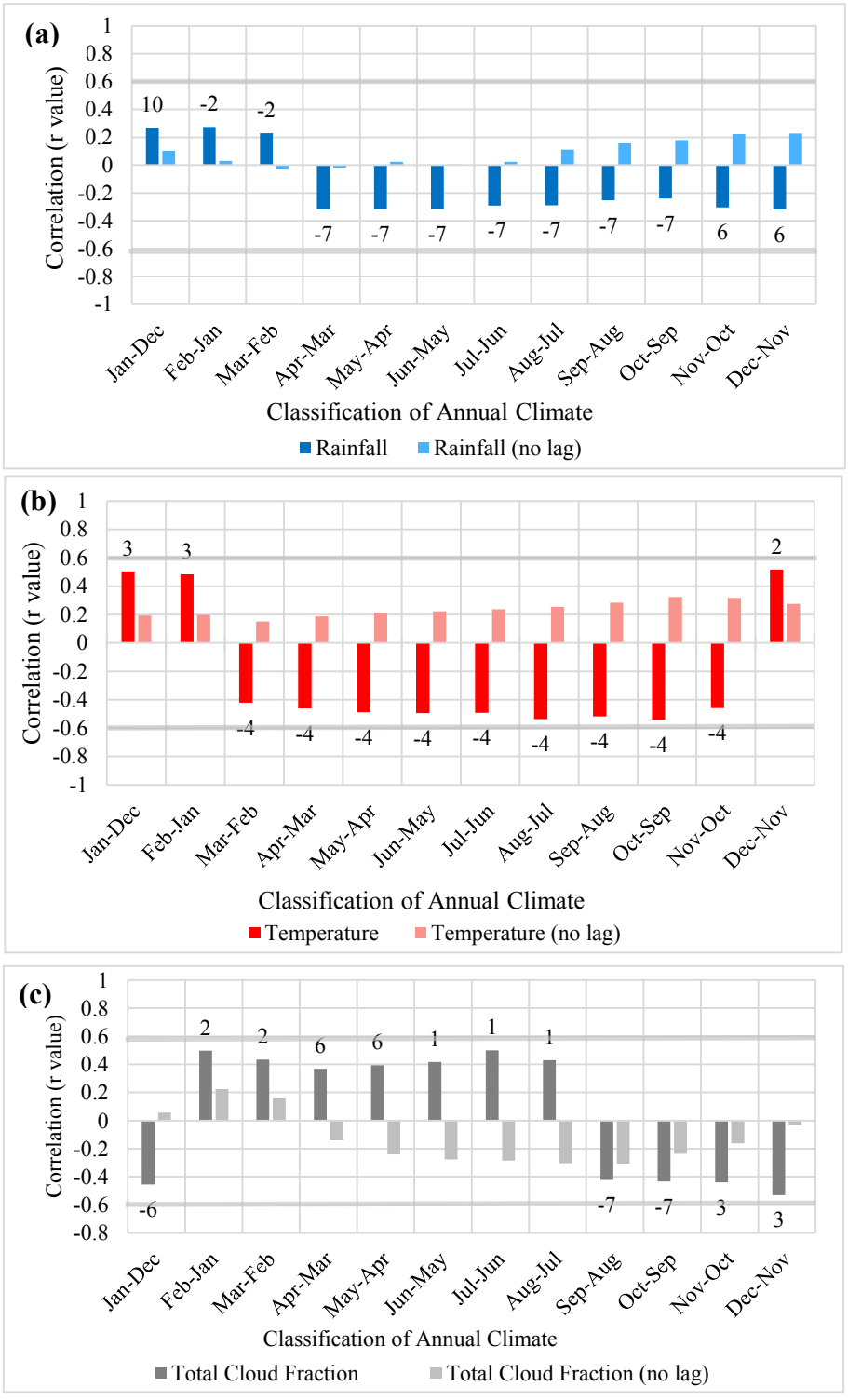

Figure 14: Correlations of *C. japonica* (Hilo Re.) Tree Ring Growth and Annual Climate Variables r values (y axis) of linear correlations between tree ring growth of composite core and rainfall **(a)**, temperature **(b)**, and total cloud fraction **(c)**. Correlations were performed for the 12 different classifications of annual climate data (x axis). In each correlation, the highest r value was selected out of lag values ranging from -10 to 10 (lag value labeled). Also, zero lag correlations are shown (lighter color). |r| > 6 (gray lines) indicate a strong correlation.

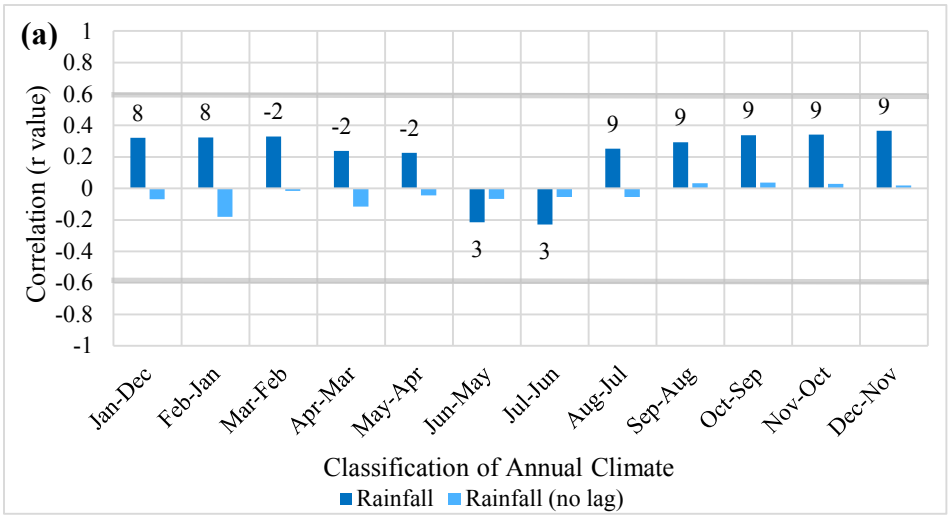

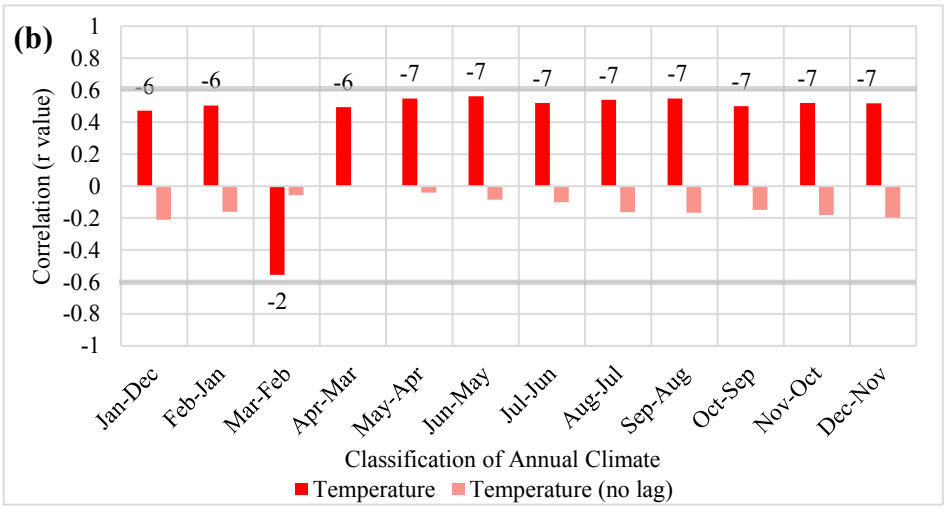

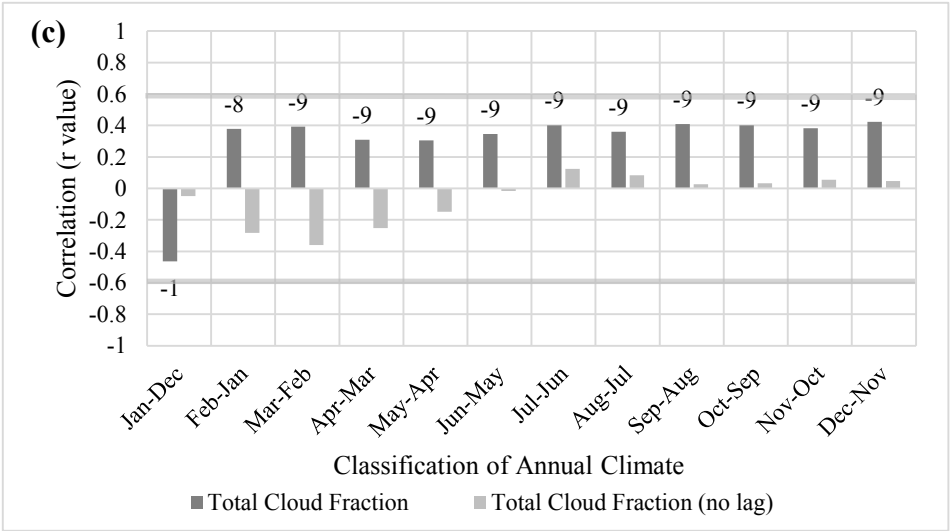

Figure 15: Correlations of *P. menziesii* (Doctor's Pit) Tree Ring Growth and Annual Climate Variables r values (y axis) of linear correlations between tree ring growth of composite core and rainfall **(a)**, temperature **(b)**, and total cloud fraction **(c)**. Correlations were performed for the 12 different classifications of annual climate data (x axis). In each correlation, the highest r value was selected out of lag values ranging from -10 to 10 (lag value labeled). Also, zero lag correlations are shown (lighter color). $|r| > 6$ (gray lines) indicate a strong correlation.

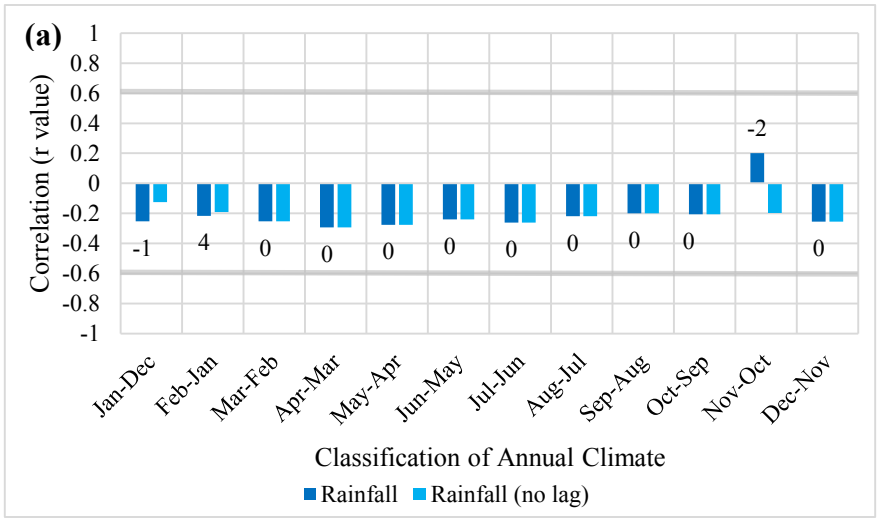

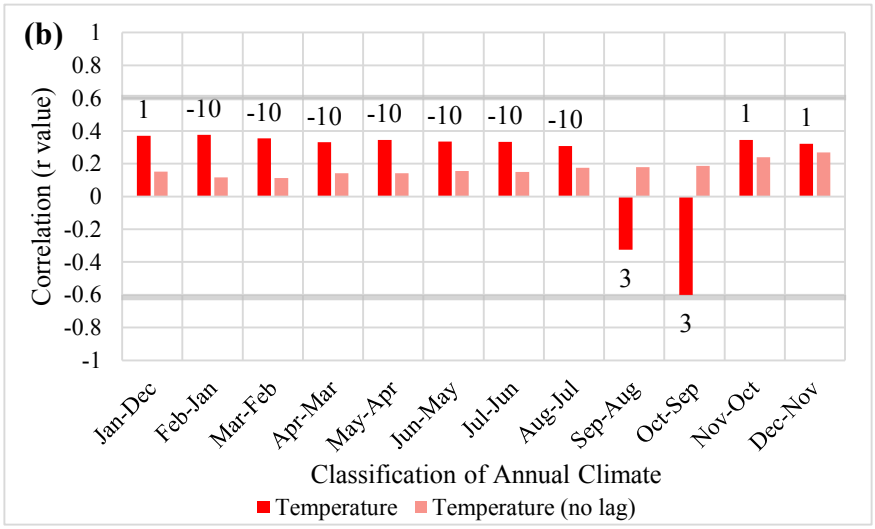

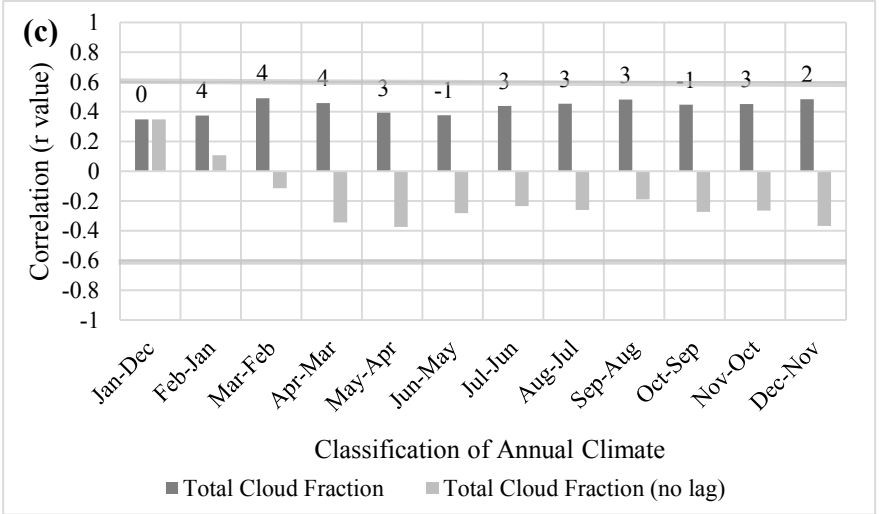

Figure 16: Correlations of *Cupressus sp.* (Doctor's Pit) Tree Ring Growth and Annual Climate Variables r values (y axis) of linear correlations between tree ring growth of composite core and rainfall **(a)**, temperature **(b)**, and total cloud fraction **(c)**. Correlations were performed for the 12 different classifications of annual climate data (x axis). In each correlation, the highest r value was selected out of lag values ranging from -10 to 10 (lag value labeled). Also, zero lag correlations are shown (lighter color). $|r| > 6$ (gray lines) indicate a strong correlation.

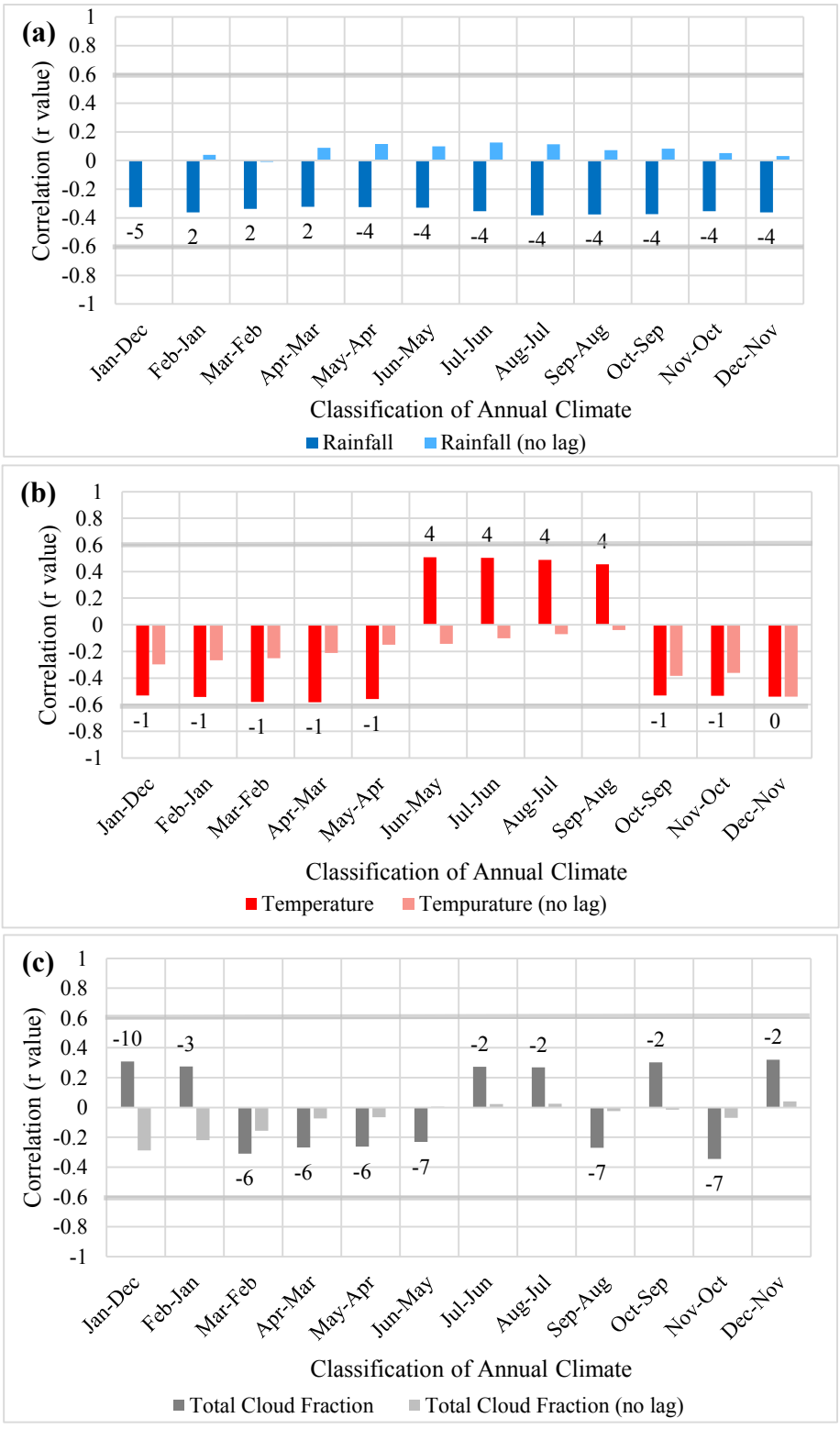

Figure 17: Correlations of *C. japonica* (Palika Ra.) Tree Ring Growth and Annual Climate Variables r values (y axis) of linear correlations between tree ring growth of composite core and rainfall **(a)**, temperature **(b)**, and total cloud fraction **(c)**. Correlations were performed for the 12 different classifications of annual climate data (x axis). In each correlation, the highest r value was selected out of lag values ranging from -10 to 10 (lag value labeled). Also, zero lag correlations are shown (lighter color). $|r| > 6$ (gray lines) indicate a strong correlation.

Next, I hypothesized that there is a positive correlation between tree ring growth and temperature, a positive correlation between tree ring growth and rainfall, and a negative correlation between tree ring growth and cloud cover. Also, I hypothesized that rainfall would have the strongest correlation with tree ring growth than with any other climate variable. To test these hypotheses, linear correlations were performed between tree ring growth of the four composite cores and time series data of three climate variables of each sampling site (temperature, rainfall, and cloud cover). Also, 12 different classifications of annual anomalous climate data and lag values ranging between -10 and 10 were utilized in each correlation.

Overall, there were no strong correlations ($|r| > 0.6$) and significant ($p > 0.05$) correlations between tree ring growth and any of the annual anomalous climate variables (Figures 14-17). Furthermore, lag values that resulted in the highest r values were not consistent throughout each correlation between tree ring growth of a composite core and the three climate variables. If lag values were consistent throughout each correlation of a composite core, then that would have indicated obvious errors in the counting and identifying of tree rings. Thus, there is insufficient evidence to suggest that tree ring growth of the sampled trees corresponded with rainfall, temperature, and cloud cover. Moreover, it was unclear how impactful errors in the counting and identifying of tree rings affected each correlation.

3.4 Multiple Linear Regression Model of Tree Ring Growth

In addition to testing for correlation between tree ring growth and climate, a multiple linear regression approach was taken to test if tree ring growth responded to a

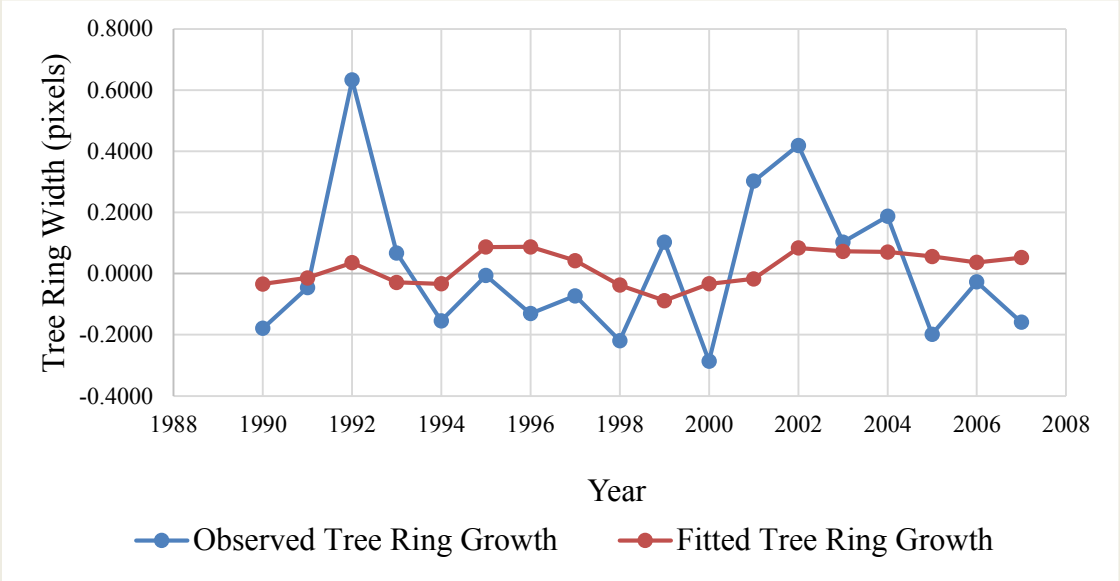

Figure 18: Multiple Linear Regression of Tree Ring Growth: *C. japonica* (Hilo Re.) Best fit values tree ring growth (y) determined by our multiple linear regression model with annual temperature (x_1), rainfall (x_2), and total cloud fraction (x_3) as independent variables.
$y = (-1.15) + (0.11)\, x_1 + (-0.001)\, x_2 + (0.12)\, x_3$ (R^2=0.05)

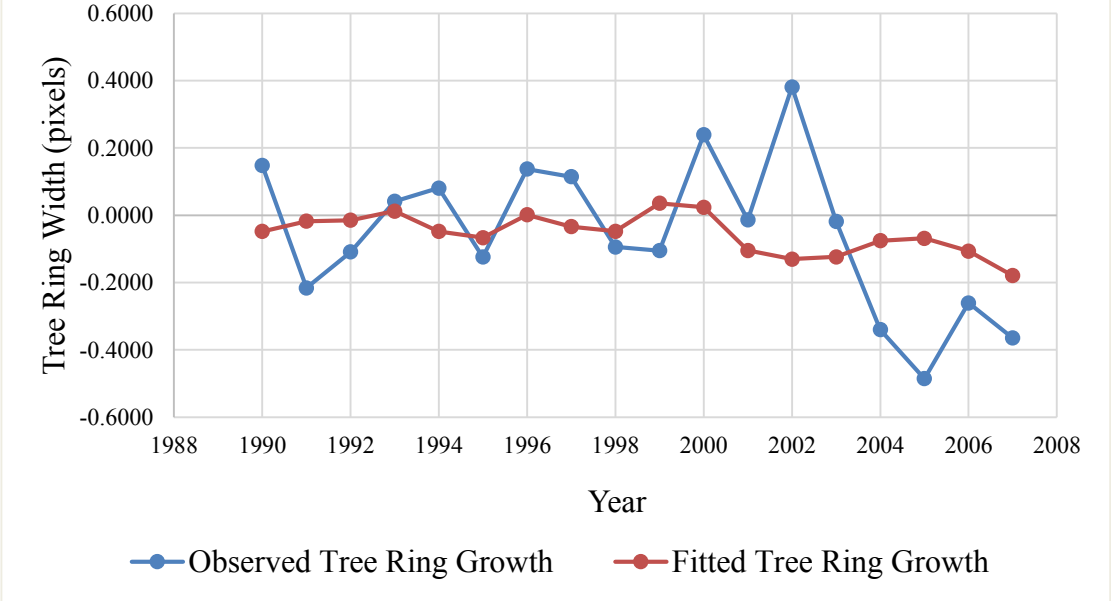

Figure 19: Multiple Linear Regression of Tree Ring Growth: *P. menziesii* (DP) Best fit values of tree ring growth (y) determined by our multiple linear regression model with annual temperature (x_1), rainfall (x_2), and total cloud fraction (x_3) as independent variables.
$y = (1.40) + (-0.04)\, x_1 + (-0.04)\, x_2 + (-2.05)\, x_3$ (R^2=0.07)

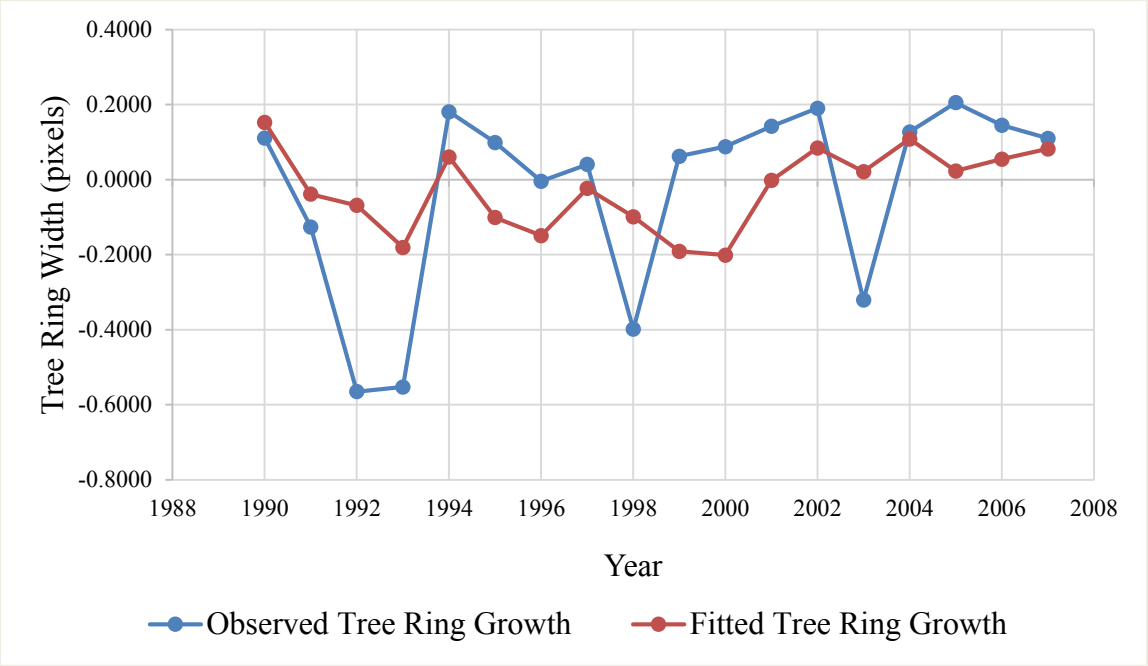

Figure 20: Multiple Linear Regression of Tree Ring Growth: *Cupressus sp.* (DP) Best fit values of tree ring growth (y) determined by our multiple linear regression model with annual temperature (x_1), rainfall (x_2), and total cloud fraction (x_3) as independent variables.
$y = (-3.17) + (0.11)\, x_1 + (-0.0002)\, x_2 + (3.23)\, x_3$ (R^2=0.18)

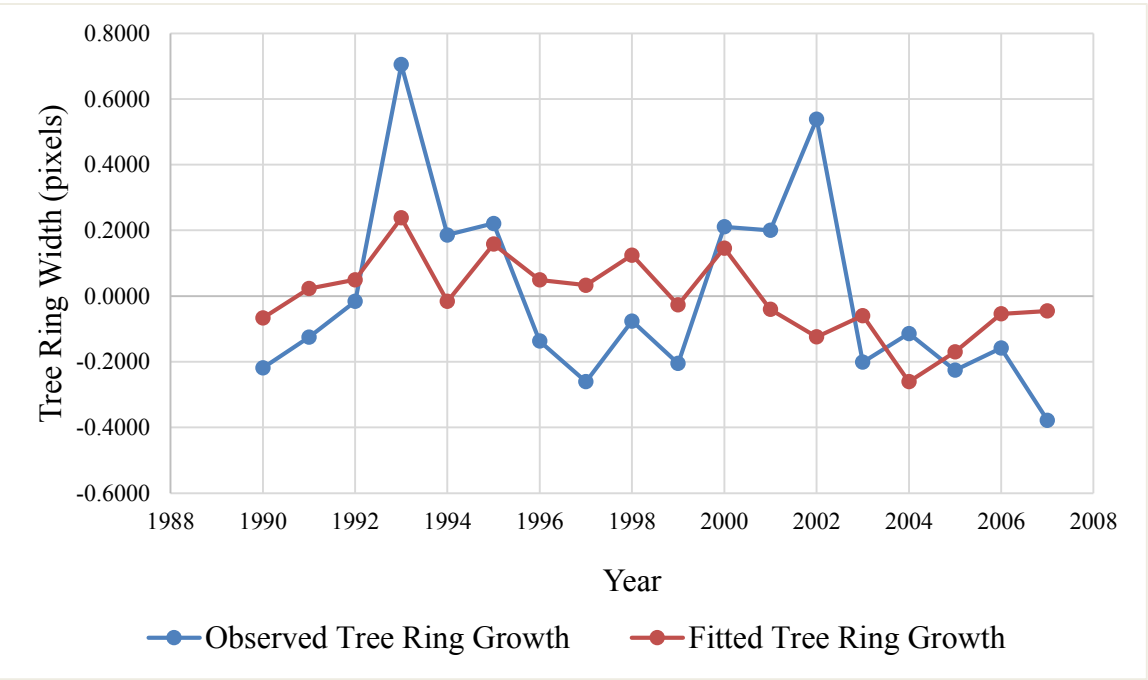

Figure 21: Multiple Linear Regression of Tree Ring Growth: *C. japonica* (Palika Ra.) Best fit values of tree ring growth (y) determined by our multiple linear regression model with annual temperature (x_1), rainfall (x_2), and total cloud fraction (x_3) as independent variables.
$y = (4.50) + (-0.13)\, x_1 + (-0.00004)\, x_2 + (-3.58)\, x_3$ (R^2=0.18)

combination of temperature, rainfall, and cloud cover. Four multiple linear regression models were constructed to produce best fit values of tree ring widths of each composite core. Y intercept and coefficient values of each independent variable (temperature, rainfall, and cloud cover) were generated. Also, R^2 values were produced in each model to indicate how well best fit values of tree ring width matched observed values of tree ring widths.

In all multiple linear regression models (Figures 18-21), best fit values of tree ring widths (red) poorly matched observed values of tree ring widths (blue), as indicated by the low R^2 values of each model (*Cryptomeria japonica,* Hilo Reserve: 0.05; *P. menziesii,* Doctor's Pit: 0.07; *Cupressus sp.,* Doctor's Pit: 0.18; *C.japonica*, Palika Ranch: 0.18). Thus, there is insufficient evidence that sampled trees from Hawai'i Island significantly responded to a combination of temperature, rainfall, and cloud cover.

3.5 Response of Tree Ring Growth During El Niño Events

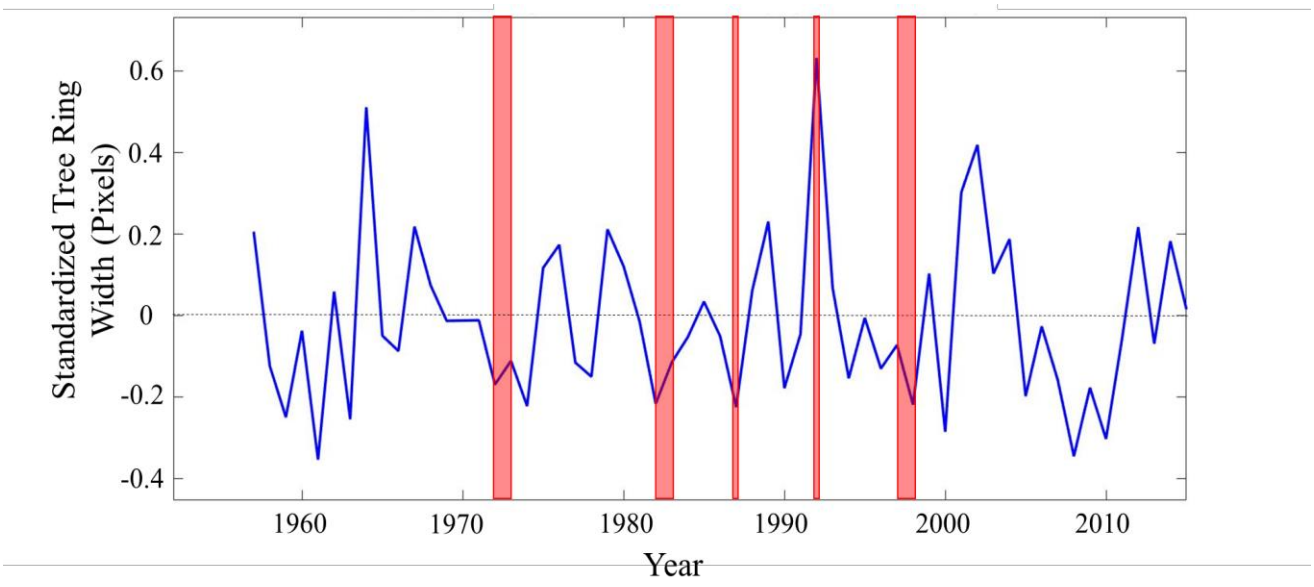

Figure 22: El Niño and Tree Ring Growth of *C. japonica* (Hilo Re.) Composite Core Positive values indicate greater than normal tree ring growth and negative values indicate below normal tree ring growth. Red shadings mark significant El Niño events (Huang et al., 2014; Liu et al., 2014; Huang et al., 2015).

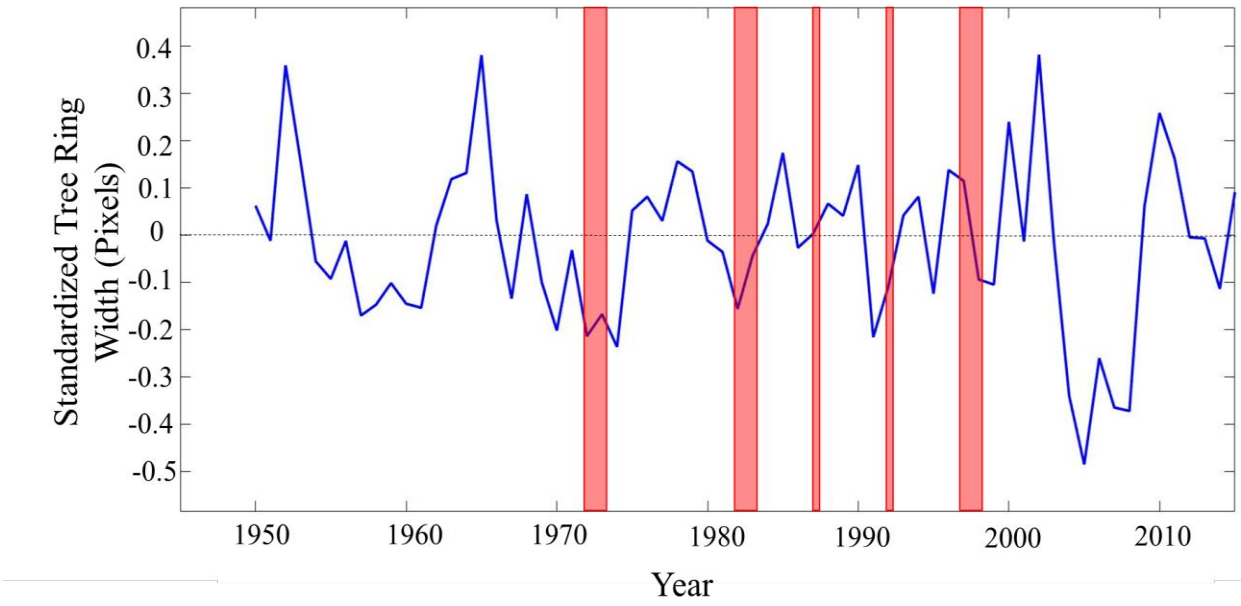

Figure 23: El Niño and Tree Ring Growth of *P. menziesii* (DP) Composite Core Positive values indicate greater than normal tree ring growth and negative values indicate below normal tree ring growth. Red shadings mark significant El Niño events (Huang et al., 2014; Liu et al., 2014; Huang et al., 2015).

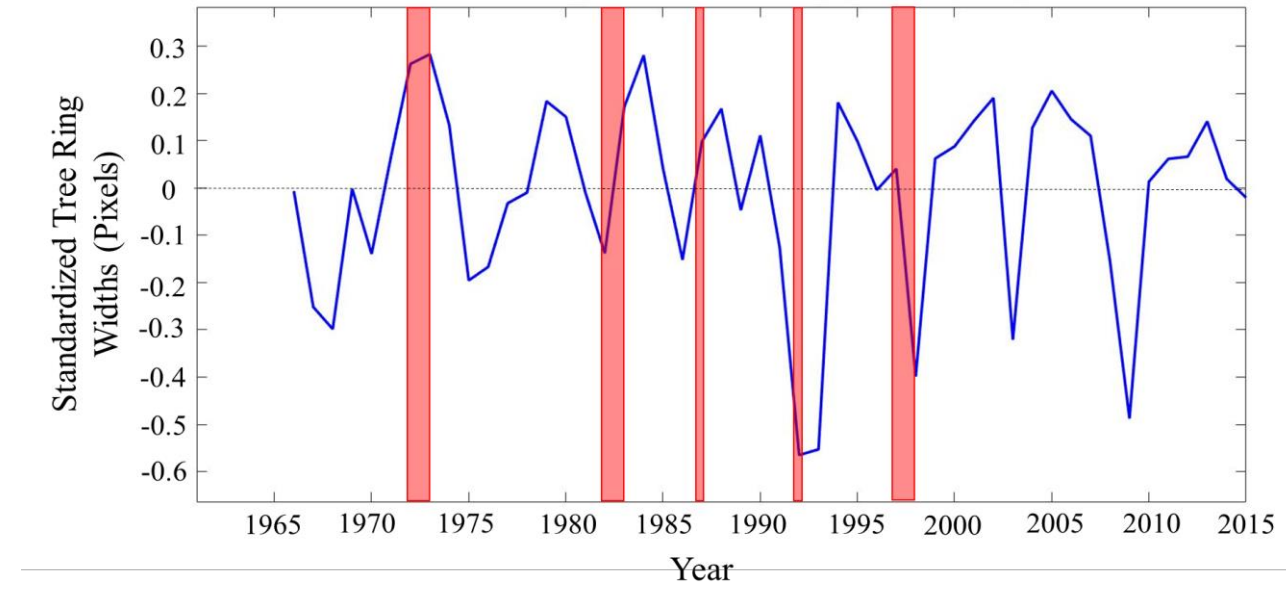

Figure 24: El Niño and Tree Ring Growth of *Cupressus sp.* (DP) Composite Core Positive values indicate greater than normal tree ring growth and negative values indicate below normal tree ring growth. Red shadings mark significant El Niño events (Huang et al., 2014; Liu et al., 2014; Huang et al., 2015).

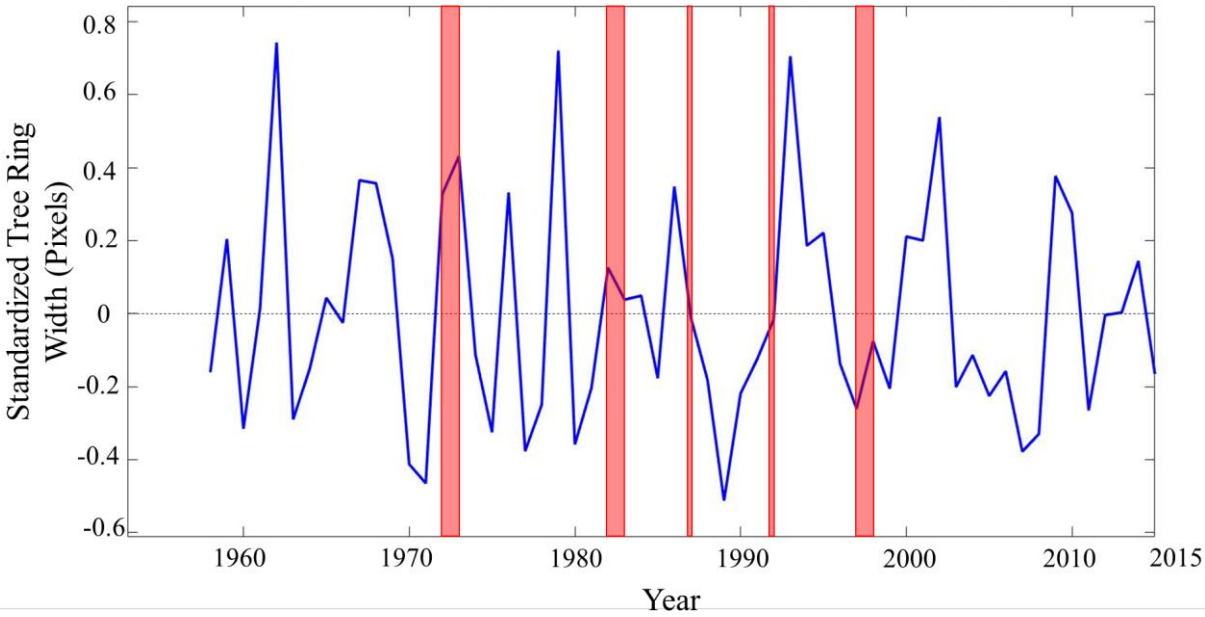

Figure 25: El Niño and Tree Ring Growth of *C.japonica* (Palika Ranch) Composite Core Positive values indicate greater than normal tree ring growth and negative values indicate below normal tree ring growth. Red shadings mark significant El Niño events (Huang et al., 2014; Liu et al., 2014; Huang et al., 2015).

Lastly, I hypothesized that tree ring growth would be reduced during El Niño events. To test this hypothesis, tree ring width values corresponding to the strongest El Niño years were examined for each composite core (Figures 22-25). Specially, any patterns or responses in tree ring growth of each composite core were assessed during the strongest El Niño events (red).

Overall, there was no consistent response in tree ring growth during El Niño events in any of the composite cores. Only during the 1998 El Niño event, below normal tree ring growth occurred in all composite cores. Tree ring growth of the *C. japonica* (Hilo Reserve) composite core and tree ring growth of the *P. menziesii* (Doctor's Pit) composite core (Figures 22 and 23 respectively) indicated modest responses of reduced tree ring growth during El Niño years. However, this was not consistent. For example, during the 1993 El Niño year, tree ring growth of the *C. japonica* (Hilo Reserve) composite core was much

larger than normal. Ultimately, it is inconclusive if tree ring growth responded to El Niño events in Hawai‘i.

4.0 DISCUSSION

4.1 Conifers in Hawai‘i Show Promise as a Proxy for Climate Reconstruction

When assessing the feasibility of dendrochronology in Hawai‘i, it is important to investigate if certain trees can produce annual tree rings. In this study, 6 sampled coniferous trees collected at three sites in Hawai‘i Island were analyzed for annularity in tree rings. Two out of the 6 sampled trees used in this analysis (33%) had matching years of observed and expected first growth (Figure 12). Thus, my hypothesis that trees in Hawai‘i can produce annual tree rings was supported. Furthermore, this result suggests that certain trees (specifically *Cryptomeria japonica*) are potentially useful for dendrochronological studies in Hawai‘i. It is important to note, however, that only 6 trees were tested for annual tree ring growth and other *C. japonica* trees tested in this analysis did not display annual tree ring growth. Ultimately, future dendrochronological studies in Hawai‘i should consider a larger sample size, multiple sites, and other tree species.

As for the majority of the sampled trees that did not indicate annual tree ring growth, one possible reason could be that data specified in the forestry logs were insufficient. In fact, Skolmen (1980) acknowledged that majority of the planting locations recorded in the forestry spanned a broad area. Thus, finding the exact trees sampled in this study was at best, an approximation. Second, there was probably missing data in the forestry logs. A good example of this was the lack of listed planting dates of *P. menziesii* trees at the Doctor’s Pit site. Since one year was only listed as the planting year for *P. menziesii* trees at the Doctor’s Pit site, it is not surprising that none of the sampled *P. menziesii* tree cores had years of observed first tree growth match the expected year of first

tree growth. Thus, with more details in the forestry logs, a refined analysis would have provided more accurate results.

Another possible reason why 4 out of the 6 sampled trees did not have matching years of observed and expected first growth is errors in identifying and counting tree rings. This error, explained in more detail later, would have skewed the analysis since missing or added annual tree rings in a core would have resulted in inaccurate years of observed first growth. This is probably why one of the two cores sampled from a *C. japonica* tree in Hilo Reserve had matching observed and expected years of first growth and the second core taken from the same tree did not have matching years of observed and expected first growth.

In addition to insufficient data in the forestry logs and misidentification of tree rings, the last possible reason why majority of the tree cores had mismatching years of observed and expected first growth is that 2nd generation trees of the original planted conifers were probably sampled. Since the forestry logs only recorded dates when the original conifers were planted, there is a good chance that the offspring of the original planted trees were sampled. Figure 12 shows that all mismatching tree cores (8 out of the 10 tree cores) have years of observed first growth date later than the expected years of first growth. If majority of the tree cores were sampled from 2nd generation trees, ultimately it is inconclusive whether these sampled conifers produced annual tree rings.

Along with assessing annual tree ring production, another important aspect of dendrochronology is comparing tree ring growth of different trees. If different trees share similar variations in tree ring growth, then there is a strong indication that the trees responded to the same environmental influence. In this study, there was an indication that

tree ring growth of two composite cores (*C. japonica* - Hilo Reserve) and *P. menziesii* - Doctor's Pit) corresponded (Figure 13). Because both composite cores were from two nearby windward sites, there is good indication that *C. japonica* and *P. menziesii* trees at both windward sites responded to the same environmental influence. However, the specific environmental influence that these trees responded to is unknown. Nevertheless, this suggests that *C. japonica* and *P. menziesii* are potentially useful trees for dendrochronological studies in Hawai'i.

4.2 Relationships Between Climate and Tree Growth?

The next important step in assessing the feasibility of dendrochronology in Hawai'i is to investigate the relationship between tree ring growth and climate. I hypothesized that there is a positive correlation between rainfall and tree ring growth, a positive correlation between temperature and tree ring growth, and a negative correlation between cloud cover and tree ring growth. However, there were no strong or significant correlations ($|r| < 0.6$, $p > 0.05$) between any of the climate variables and tree ring growth of the composite cores (Figures 14-17). Furthermore, all linear correlations used in this analysis included all possible yearly periods of tree ring growth, but still no significant correlation values emerged. Thus, not only were my previous hypotheses unsupported, but my other hypothesis that rainfall would have the strongest correlation with tree ring growth than any other climate variable was also unsupported. In fact, despite all insignificant r values, rainfall seemed to have relatively low r values compared to the r values of temperature and cloud cover. The results in this study were in contrast to Francisco et al. (2015), where they found that annual tree ring growth of *Sophora chrysophylla* growing in Pohakuloa (Hawai'i

Island) was significantly correlated to rainfall. This suggests that conifers in Hawai‘i Island respond differently to rainfall compared to the non-coniferous *Sophora chrysophylla.*

Next, multiple linear regression models were constructed to test if tree ring growth of the sampled trees was a response to temperature, rainfall, and cloud cover. Though this approach is closely related to the correlation approach applied previously, a multiple linear regression approach statistically examined how influential a combination of temperature, rainfall, and cloud cover was to the production of annual tree rings of the sampled trees. If temperature, rainfall, and cloud cover were significant drivers of annual tree ring production, then best fit tree ring width values produced by the multiple linear regression models would have matched observed tree ring width values. However, since best fit tree ring width values poorly matched the observed tree ring width values for all composite cores (indicated by the low R^2 values), there was no indication that sampled trees responded to temperature, rainfall, or cloud cover.

Perhaps it is not surprising that a significant relationship between climate and tree ring growth was not found from the multiple linear regression approach, given that all correlations between tree ring growth and the climate variables were not significant. Despite unsupportive evidence in this study, I want to emphasize that this does not mean there is no possible relationship between annual tree ring growth in Hawai‘i and climate.

At best, the relationship between tree ring growth and climate in Hawai‘i interact in a way that the methods used in this study did not account for. For example, climate drivers of annual tree ring production could change as the tree ages. In other words, it could be possible that rainfall is the main factor of annual tree ring growth when the tree is in its early stages of growth. But as the tree ages, temperature may become the main factor of

annual tree ring growth. Also, the relationship between tree ring growth and climate can become complicated due to a dampening effect between intra-annual rainfall and temperature. For example, at the Palika Ranch site, the typical wet period occurs during the typical cold period (Figure 2a,b). This situation may counter any strong seasonal variations needed for the production of annual tree ring.

Next, the following are other possibilities that can be studied in order to further investigate the relationship between tree ring growth and climate in Hawai‘i. First, since seasonality has such a critical role in the production of annual tree rings, one thing that could be tested is how significant the variation ratio of annual seasonality (i.e. rainfall or temperature) is on tree ring growth in Hawai‘i. Or, another thing to test for is a correlation between tree ring growth and climate (i.e rainfall and temperature) only during certain periods of the year (i.e. wet and warm months experienced at the sampling site). Conversely, future investigations should examine if tree ring growth responds only to strong variations in climate on inter-annual time scales. And lastly, there could be unknown factors, possibly not related to climate (i.e. changes in nutrients), that could be influencing the production of annual tree rings in Hawai‘i. Since the linear correlation and multiple linear regression approaches used in this study did not account for any of these possible scenarios, future dendrochronological studies in Hawai‘i are necessary. Ultimately, no matter what direction future dendrochronological studies in Hawai‘i take, it can only improve our understanding of the interaction between environment and tree growth in Hawai‘i.

4.3 Relationship Between El Niño and Tree Ring Growth?

Since reduced rainfall typically occurs in Hawai‘i during El Niño years (Chu, 1995), I hypothesized that tree ring growth would have been reduced during El Niño years. However, there was no consistent response of reduced tree ring growth (or any consistent response for that matter) during the strongest El Niño years. Thus, my hypothesis was not supported. Because tree ring growth did not seem to respond to any of the three climate variables (temperature, rainfall, and cloud cover) as tested through a linear correlation approach and a multiple linear regression approach, it is not surprising that the sampled trees did not respond to the El Niño phenomena. Ultimately, El Niño events may impact tree ring growth in Hawai‘i, but a better understanding of the relationship between tree ring growth and climate in Hawai‘i is required.

4.4 Sources of Error

Throughout this study, multiple methods were used to assess the feasibility of dendrochronology in Hawai‘i. However, in each method, it is important to consider the inherent sources of the error. Hopefully, future dendrochronological studies in Hawai‘i can account for these particular errors.

One of the largest sources of error was the identification and demarcation of tree ring boundaries during the digitization of our tree cores. This subjective process required much patience and skill to analyze each tree ring boundary and to trace each tree ring boundary onto each tree core image. Especially when tree ring boundaries were close together at the outer portions of the cores due to the aging effect, the identification of the tree ring boundaries became increasingly difficult. Obviously, errors in the marking of tree ring boundaries would have resulted in errors in the counting and measurement of tree ring

widths. Thus, the results of this study are probably skewed due to incorrect counts and inaccurate measurements of tree ring widths.

In each linear correlation between the three climate variables and tree ring growth of the composite cores, the best correlation values out of lag values ranging from -10 to 10 were selected to compensate for this particular error. Since the true amount of counting errors in each of the tree cores was not known, the best correlation value out the range of lags was selected due to the assumption that the best correlation value would emerge and correspond to the true amount of tree rings in each composite core. However, by selecting the best correlation value, other sources of error were inherited. In particular, selecting the best correlation value possibly eliminated the true correlation value, which may not have been the strongest correlation out of the range of lags. Ultimately, the best solution to address this issue is to recount and reanalyze each tree ring boundary. Moreover, recounting and reanalyzing tree ring boundaries would provide a better indication of how much error occurs in tree ring identification process. In the end, with more experience of analyzing tree cores and experimentation with other analyzation techniques, the occurrences of these errors will be reduced.

Another source of error may be due to non-climatic influences affecting the tree growth of the sampled tree. For example, the occurrence of false tree rings, diseases, fires, pests, or just natural tree ring width variations produced by the tree itself, all could have led to inaccurate counts and measurements of tree rings. In this study, composite cores were created to best minimize these non-climatic influences. By averaging each width value to construct our composite cores, non-climatic errors of each sampled core were reduced.

5.0 CONCLUSION

In this study, there was an indication that coniferous trees (*Cryptomeria japonica*) in Hawai‘i can produce annual tree rings. However, a larger sample size, more tree species sampled, better records in the forestry logs, and reduced errors in identifying and counting tree rings can better support this conclusion. Also, there was an indication that tree ring growth of *C. japonica* trees at the Hilo Reserve and tree ring growth of *P. menziesii* trees at the Doctor's Pit were in correspondence. This suggested that these two species of trees located near each other possibly responded to the same environmental influence. Thus, these two species are potentially useful for future dendrochronological studies in Hawai‘i.

After performing linear correlations and multiple linear regression models, it is inconclusive if variations in tree ring growth in Hawai‘i is a response to variations in temperature, rainfall, and cloud cover. Also, there were no observable responses in tree ring growth during the strongest El Niño events. To conclude, dendrochronology can be an applicable approach to reconstructing climate in Hawai‘i, however, the exact relationship between tree ring growth and climate in Hawai‘i needs to be further investigated.

APPENDIX 1

Rainfall of Rain Gauge Stations Rainfall values recorded by rain gauge stations utilized for correlations. Details of rain gauge stations are found in Table 2. Rainfall data provided by Giambelluca et al. (2013) and Frazier et al., (2016).

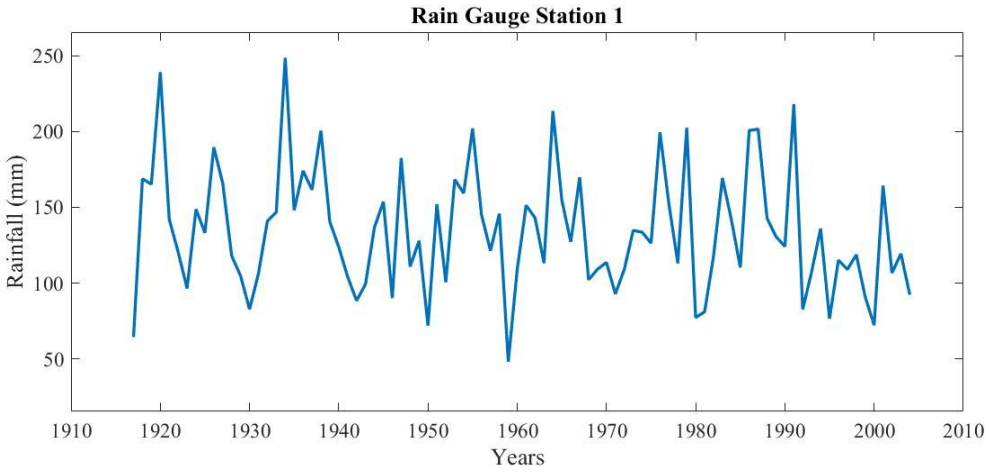

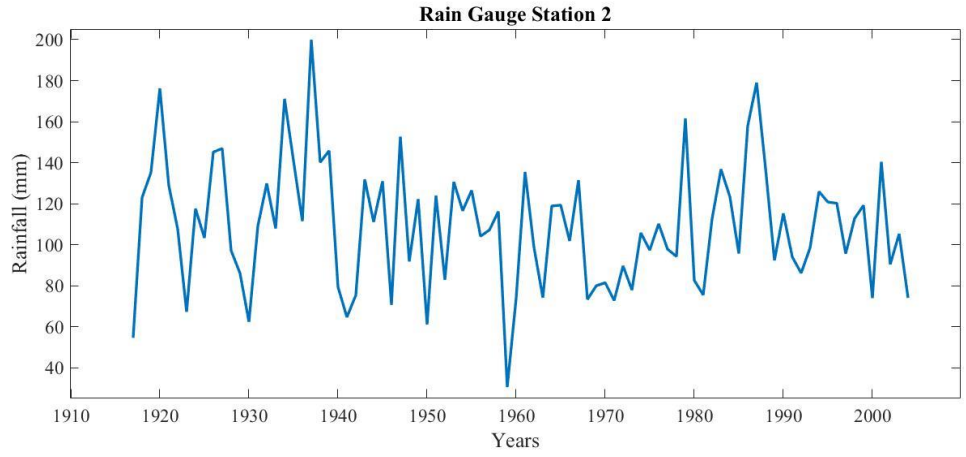

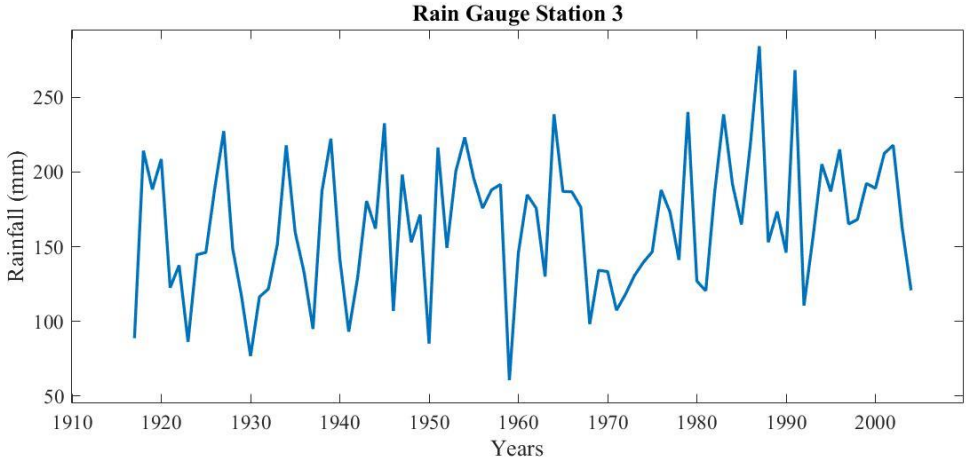

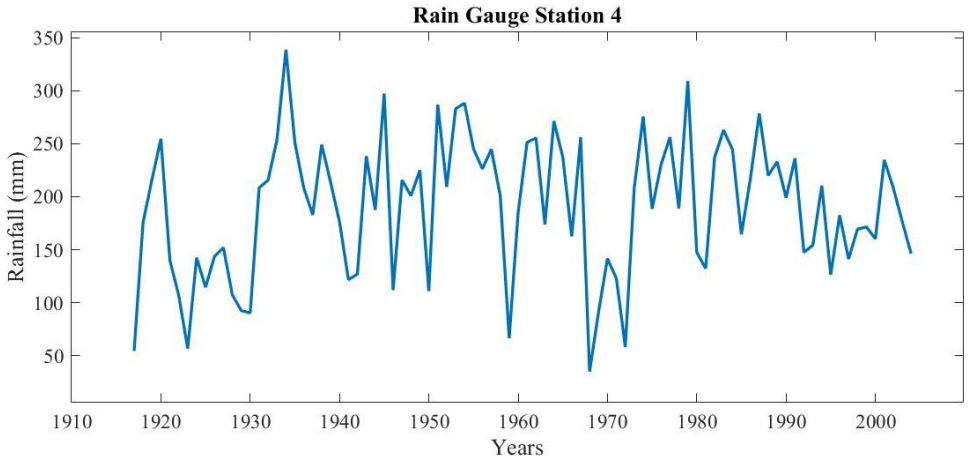
Rain Gauge Station 4
Rainfall (mm)
350
300
250
200
150
100
50
1910
1920
1930
1940
1950
1960
1970
1980
1990
2000
Years

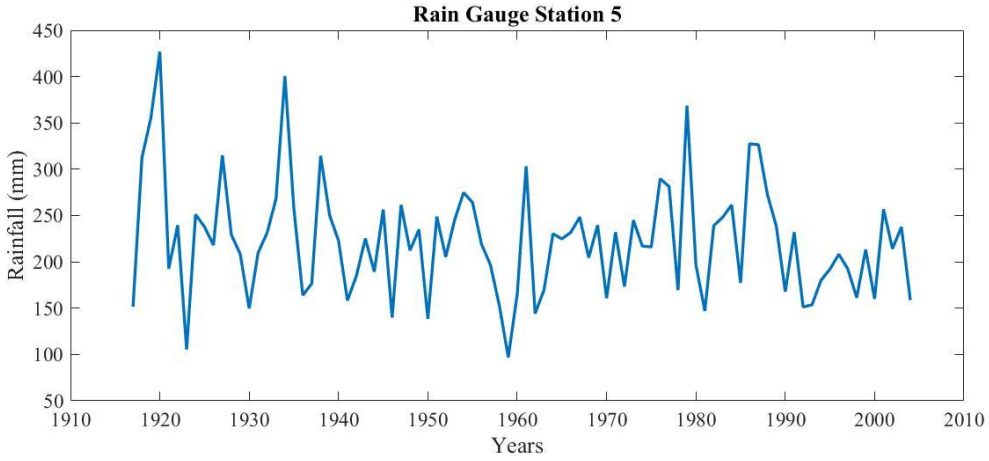
Rain Gauge Station 5
Rainfall (mm)
450
400
350
300
250
200
150
100
50
1910
1920
1930
1940
1950
1960
1970
1980
1990
2000
2010
Years

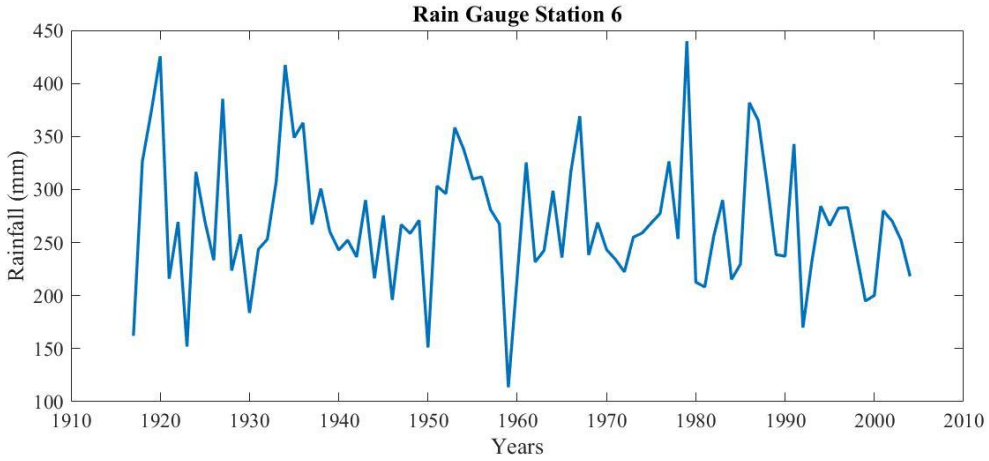
Rain Gauge Station 6
Rainfall (mm)
450
400
350
300
250
200
150
100
1910
1920
1930
1940
1950
1960
1970
1980
1990
2000
2010
Years

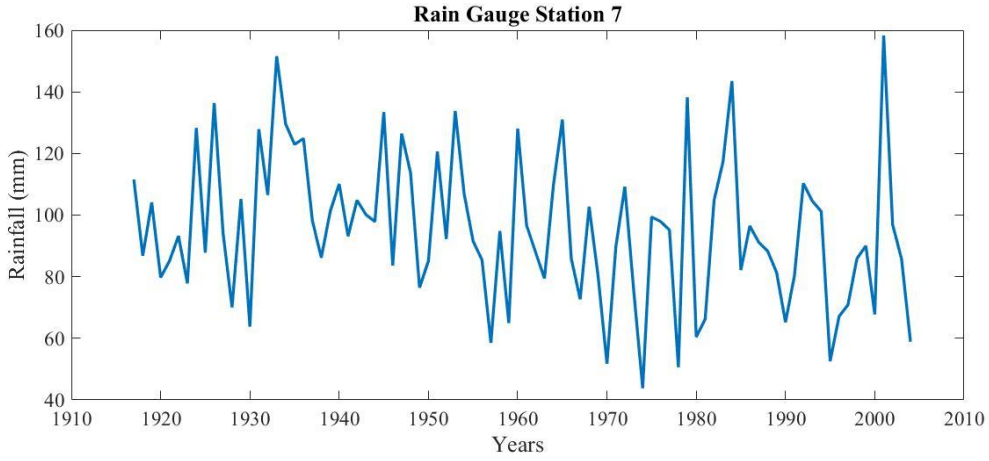
Rain Gauge Station 7
Rainfall (mm)
Years
160
140
120
100
80
60
40
1910
1920
1930
1940
1950
1960
1970
1980
1990
2000
2010

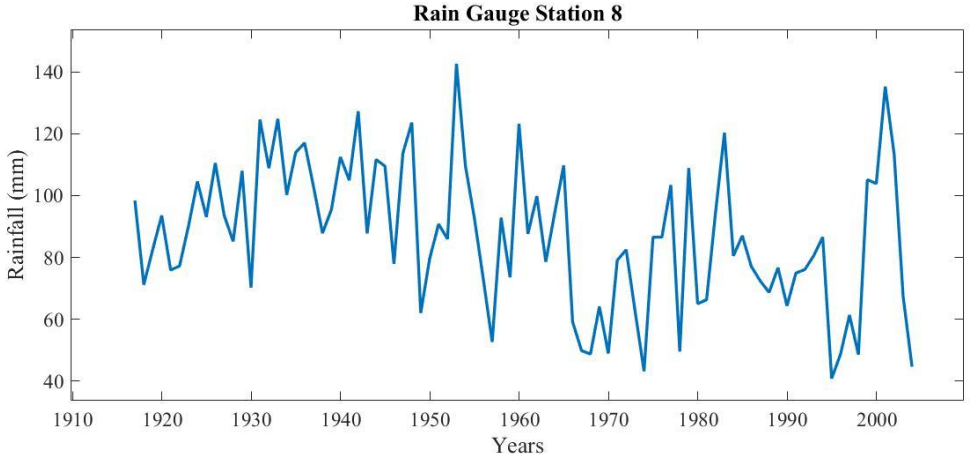
Rain Gauge Station 8
Rainfall (mm)
Years
140
120
100
80
60
40
1910
1920
1930
1940
1950
1960
1970
1980
1990
2000

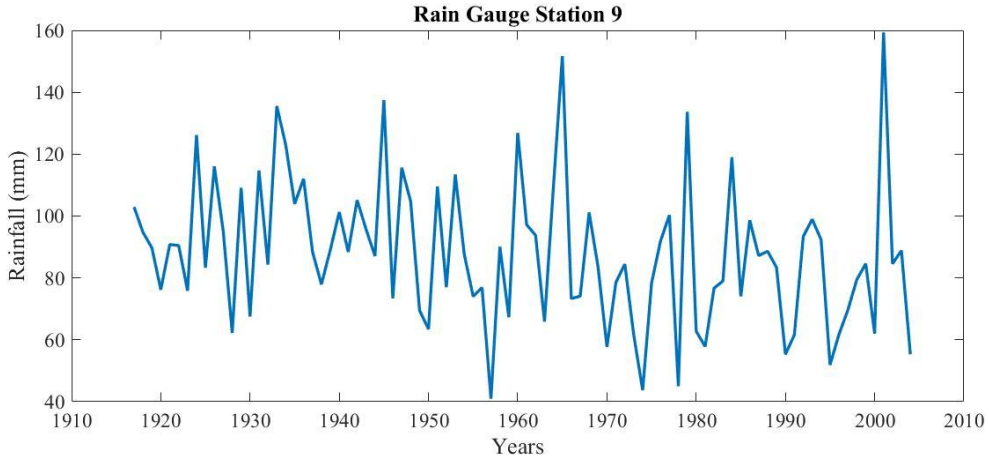
Rain Gauge Station 9
Rainfall (mm)
Years
160
140
120
100
80
60
40
1910
1920
1930
1940
1950
1960
1970
1980
1990
2000
2010

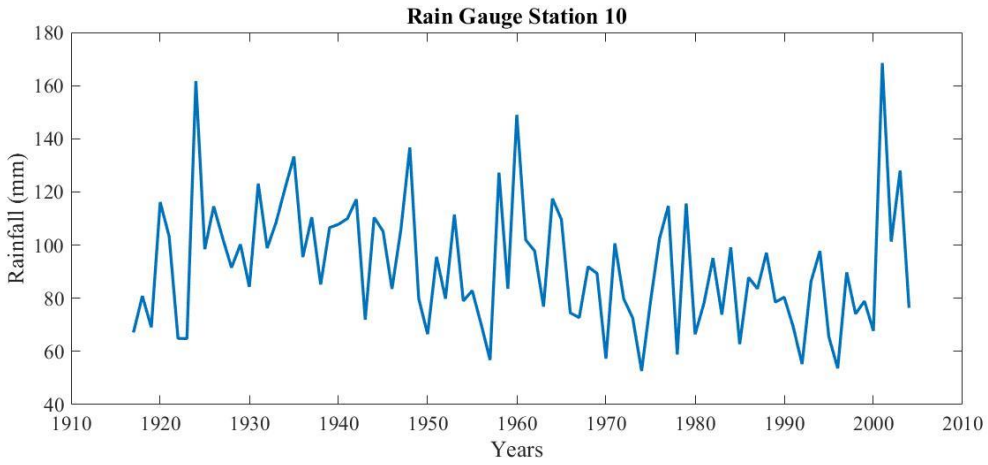
Rain Gauge Station 10
Rainfall (mm)
Years
180
160
140
120
100
80
60
40
1910
1920
1930
1940
1950
1960
1970
1980
1990
2000
2010

Literature Cited

Brienen, R. & Zuidema, P. (2005). Relating tree growth to rainfall in Bolivian rain forests: a test for six species using tree ring analysis. *Oecologia*. 146(1). pg. 1-12.

Chen, H. & Chu, P.S. (2005). Interannual and interdecadal rainfall variations in the Hawaiian Islands. *Journal of Climate.*18. pg. 4796-4813.

Chu, P.S. (1995). Hawai‘i rainfall anomalies and El Niño. *Journal of Climate*. 8. pg. 1697–1703.

Cook, E. & Jacoby, G. (1977). Tree-ring-drought relationships in the Hudson Valley, New York. *Science.* 198(4315). pg. 399-401.

Diaz, H. & Giambelluca, T. (2012). Changes in atmospheric circulation patterns associated with high and low rainfall regimes in the Hawaiian Islands region on multiple time scales. *Global and Planetary Change.* 98-99. pg. 97-108.

Fortini, L., Price, J., Jacobi, J., Vorsino, A., Burgett, J., Brinck, K., Amidon, F., Miller, S., Gon, S., Koob, G., and Paxton, E. (2013). A landscape-based assessment of climate change vulnerability for all native Hawaiian plants. *Hawai‘i Cooperative Studies Unit Technical Report.*

Francisco, K., Hart, P., Li, J., Cook, E., Baker, P. (2015). Annual rings in a native Hawaiian tree, *Sophora chrysophylla*, on Maunakea, Hawai‘i. *Journal of Tropical Ecology.* 31(6). pg. 567 – 571.

Frazier, A. G., Giambelluca, T. W., Diaz, H. F. and Needham, H. L. (2016). Comparison of geostatistical approaches to spatially interpolate month-year rainfall for the Hawaiian Islands. *International Journal of Climatology.* 36(3). pg. 1459-1470.

Giambelluca, T.W., Chen, Q., Frazier, A.G., Price, J.P., Chen, Y.-L., Chu, P.-S., Eischeid, J.K., Delparte, D.M. (2013). Online rainfall atlas of Hawai‘i. *Bull. Amer. Meteor. Soc.* 94. pg. 313-316.

Gonzalez-Elizondo, M., Jurado, E., Navar, J., Gonzalez-Elizondo, M., Villanueva, J., Aguirre, O., Jimenez, J. (2005). Tree-rings and climate relationships for Douglas-fir chronologies from the Sierra Madre Occidental, Mexico: A 1681–2001 rain reconstruction. *Forest Ecology and Management*. 213(1-3). pg. 39-53.

Griffin, D., Meko, D., Touchan, R., Leavitt S., Woodhouse, C. (2011). Latewood chronology development for summer-moisture reconstruction in the US Southwest. *Tree-Ring Research.* 6(2). pg. 87-101.

Grissino-Mayer, H. (1993). An updated list of species used in tree-ring research. *Tree-Ring Bulletin*. 53. pg. 17-53.

Grissino-Mayer, H. (2003). Manual and tutorial for the proper use of an incremental borer. *Tree-Ring Research*. 59(2). pg. 63-79.

Huang, B., Banzon, V.F., Freeman, E., Lawrimore, J., Liu, W., Peterson, T.C., Smith, T.M., Thorne, P.W., Woodruff, S.D., Zhang, H.-M. (2014) Extended Reconstructed Sea Surface Temperature version 4 (ERSST.v4): Part I. Upgrades and intercomparisons. *Journal of Climate*. in press.

Liu, W., Huang, B., Thorne, P.W., Banzon, V.F., Zhang, H.-M., Freeman, E., Lawrimore, J., Peterson, T.C., Smith, T.M., Woodruff, S.D. (2014) Extended Reconstructed Sea Surface Temperature version 4 (ERSST.v4): Part II. Parametric and structural uncertainty estimations. *Journal of Climate*. in press.

Huang, B., Thorne, P., Smith, T., Liu, W., Lawrimore, J., Banzon, V., Zhang, H., Peterson, T., Menne, M. (2015). Further exploring and quantifying uncertainties for Extended Reconstructed Sea Surface Temperature (ERSST) Version 4 (v4). *Journal of Climate.* in press.

Lawrimore, J. H., Menne, M. J., Gleason, B. E., Williams, C. N., Wuertz, D. B., Vose, R. S., Rennie, J. (2011). An overview of the Global Historical Climatology Network monthly mean temperature dataset, version 3. *Journal of Geophysical Research*. 116. pg. D19121.

Li, J., Xie1, S.-P., Cook, E., Huang, G., D'Arrigo, R., Liu, F., Ma, J., Zheng, X.-T. (2011). Interdecadal modulation of El Niño amplitude during the past millennium. *Nature Climate Change.* 1. pg. 114-118.

Little Jr., E., & Skolmen, R. (1989). Common forest trees of Hawai'i. *USDA Agricultural Handbook No. 679.*

NOAA, National Center for Environmental Information. (2015). Equatorial Pacific sea surface temperature.*Website.* https://www.ncdc.noaa.gov/teleconnections/enso/indicators/sst.php#oni

Rooney, J., Fletcher, C., Grossman, E., Engels, M., Field, M. (2004). El Nino influence on Holocene reef accretion in Hawai'i. *Pacific Science.* 58(2). pg. 305-324.

Samuelson, L.J., Eberhardt, T.L., Bartkowiak, S.M., Johnsen, K.H. (2013). Relationships between climate, radial growth and wood properties of mature loblolly pine in Hawai'i and a northern and southern site in the southeastern United States. *Forest Ecology and Management*. 310. pg. 786–795.

Skolmen, R. (1980). Plantings of forest reserves in Hawai'i, 1910-1960. *Institute of Pacific Islands Forestry*. Pacific Southwest Forest and Range Experiment Station, U.S. Forest Service. Honolulu, HI.

Stahle, D. (1999). Useful strategies for the development of tropical tree-ring chronologies. *IAWA Journal*. 20(3). pg. 249-253.

Taliaferro, W. (1961). A key to climatological observations in Hawai‘i. *Weather Bureau, U.S. Department of Commerce.* Washington D.C.

Uchikawa, J., Popp, B., Schoonmkaer, J., Timmerman, A., Lorenz, S. (2010). Geochemical and climate modeling evidence for Holocene aridification in Hawai‘i dynamic response to a weakening equatorial cold tongue. *Quaternary Science Reviews.* 29. pg. 3057-3066.

U.S. National Archives and Records Administration (USNARA). (2014). e-CFR: Title 50: Wildlife and fisheries part 17-endangered and threatened wildlife and plants subpart B—lists. Electron Code Fed Regul.

Vorsino A., Fortini L., Amidon F., Miller S., Jacobi S., Price J., Gon, III, S., Koob G. (2014). Modeling Hawaiian ecosystem degradation due to invasive plants under current and future climates. *PLoS ONE*. 9(7). pg. e102400.

Woodhouse, C., Lukas, J., and Brown, P. (2002) Drought in the western Great Plains, 1845–56. *American Meteorological Society.* 83(10). pg. 1485-1493.

Worbes, M. (1999). Annual growth rings, rainfall-dependent growth and long-term growth patterns of tropical trees from the Caparo forest reserve in Venezuela. *Journal of Ecology.* 87. pg. 391-403.

Worbes, M. (2002) One hundred years of tree-ring research in the tropics, a brief history and an outlook to future challenges. *Dendrochronologia.* 20(1). pg. 217-231.

Zhang, C., Wang, Y., Hamilton, K., Lauer, A. (2016). Dynamical downscaling of the climate for the Hawaiian Islands Part I: Present-day. *Journal of Climate.* in press.

Ziegler A. (2002). Hawaiian natural history, ecology, and evolution. *University of Hawai‘i Press.* Honolulu, HI. pg. 157-182, 358-373.